OSU-TA-7/96

LOCAL LAGRANGIAN APPROXIMATIONS FOR THE EVOLUTION OF THE DENSITY DISTRIBUTION FUNCTION IN LARGE-SCALE STRUCTURE

Zacharias A.M. Protogeros and Robert J. Scherrer
Department of Physics
The Ohio State University
Columbus, OH 43210

ABSTRACT

We examine local Lagrangian approximations for the gravitational evolution of the density distribution function. In these approximations, the final density at a Lagrangian point $\mathbf{q}$ at a time t is taken to be a function only of t and of the initial density at the same Lagrangian point. A general expression is given for the evolved density distribution function for such approximations, and we show that the vertex generating function for a local Lagrangian mapping applied to an initially Gaussian density field bears a simple relation to the mapping itself. Using this result, we design a local Lagrangian mapping which reproduces nearly exactly the hierarchical amplitudes given by perturbation theory for gravitational evolution. When extended to smoothed density fields and applied to Gaussian initial conditions, this mapping produces a final density distribution function in excellent agreement with full numerical simulations of gravitational clustering. We also examine the application of these local Lagrangian approximations to non-Gaussian initial conditions.

1 INTRODUCTION

A variety of statistics have been developed to describe the evolution of the large-scale matter distribution in the universe. Among these is the one-point probability distribution function (PDF) of the density field, $P(\rho)$, which gives the probability that the density at a random point in space lies between ρ and $\rho+d\rho$. In the linear regime, the entire density field is simply scaled up the growth factor $D(t)$, so $P(\rho)$ (with ρ suitably rescaled) remains constant. In the nonlinear regime, however, $P(\rho)$ evolves in a complex manner. A number of recent studies have examined the evolution of the PDF of the density field during gravitational clustering in the nonlinear regime. Kofman (1991), Kofman et al. (1994), and Bernardeau & Kofman (1995) used the Zel'dovich approximation and the condition of mass conservation to derive an approximate expression for $P(\rho)$. Padmanabhan & Subramanian (1993) derived an approximation to the smoothed PDF from the Zel'dovich approximation. Juszkiewicz et al. (1994) used the Edgeworth expansion along with the moments of the evolved distribution to obtain an approximation for the evolved PDF (see also Bernardeau & Kofman 1995.) [For a recent review of approximation methods in general, see Sahni & Coles 1995].

All of these approximations assume Gaussian initial conditions; much less is known about the evolution of the PDF for non-Gaussian initial conditions. A number of numerical simulations have been performed to investigate the evolution of the density field in various non-Gaussian toy models (Messina et al. 1990; Moscardini et al. 1991; Matarrese et al. 1991; Weinberg & Cole 1992; Coles et al. 1993). Fry & Scherrer (1994) examined analytically the evolution of skewness in arbitrary non-Gaussian models, and this analysis was extended to the kurtosis by Chodorowski & Bouchet (1996), but very little analytic work has been done on the evolution of the full PDF in arbitrary non-Gaussian models.

In this paper, we examine a class of approximations for the evolution of the PDF which we call "local Lagrangian approximations". By "local Lagrangian", we mean that the density at the Lagrangian point $\mathbf{q}$ at a time t is approximated as a function only of t and the initial value of $\rho(\mathbf{q})$:

$$\rho(\mathbf{q},t) = f(\rho_0(\mathbf{q}),t), \tag{1}$$

where $\rho_0(\mathbf{q}) \equiv \rho(\mathbf{q},t_0)$. [We caution the reader that the term "local" has been used in this context with a variety of different meanings]. The linear approximation, for example, is a local Eulerian mapping. The Zel'dovich approximation is a Lagrangian mapping in which the density at $\mathbf{q}$ is a function only of t and the second partial derivatives of the initial potential $\phi_0(\mathbf{q})$:

$$\rho(\mathbf{q},t) = f(\phi_{0_{ij}},t) \tag{2}$$

For certain special cases (1-dimensional collapse, spherical collapse), the Zel'dovich approximation reduces to a local Lagrangian mapping of the initial density field as given in equation (1). In fact, these cases form the basis of two of our approximations. Note that we do not require a prescription for the Lagrangian mapping $\mathbf{x}(\mathbf{q})$; all we care about is the function given in equation (1), which is sufficient to calculate the PDF $P(\rho)$. In fact, for a given mapping f in equation (1), there may not even be a Lagrangian mapping scheme which produces f; nonetheless our mapping could still provide a good approximation to the evolution of the PDF.

Our motivation for considering such mappings is two-fold: for the case of Gaussian initial conditions, it would be extremely interesting if a simple mapping of the form given in equation (1) could give an accurate description of the evolution of the density PDF. We will see that this is indeed the case. For non-Gaussian initial conditions, such a mapping would allow for the investigation of the evolution of the density PDF for a wide range of initial conditions, and it might help to answer some general questions about the evolution of such density fields. For example, in the quasi-linear regime, is there any general difference between the

rate at which $\langle\delta^2\rangle$ evolves in non-Gaussian models, versus its evolution in Gaussian models? Fry & Scherrer (1994) suggested that in the quasi-linear regime, models with positive initial skewness would have an rms density fluctuation slightly larger than that predicted by linear theory, while negative skewness models would have an rms fluctuation slightly smaller than the linear prediction. The results of Weinberg & Cole (1992) support this conclusion with regard to models with negative initial skewness but are inconclusive with regard to models with positive initial skewness. A second issue addressed by Fry & Scherrer was the evolution of skewness in non-Gaussian models. Their results suggest that the skewness of the evolved density field is sensitive to the initial kurtosis (as well as the initial skewness), but the expressions they derive contain integrals over the initial three- and four-point functions, so it is difficult to draw general conclusions about the evolution of the skewness in such models. These are some of the many important general questions about the evolution of non-Gaussian models which are at present unanswered.

In this paper, we consider three different models for the Lagrangian density mapping in eq. (1). The first of these corresponds to the exact evolution in the 1-dimensional case, and it would be exact in the case of 1-D symmetry. Our second model is based on the approximation method given by Padmanabhan & Subramanian (1993), and it corresponds to the Zel'dovich approximation for spherically-symmetric collapse. We believe that the correct PDF will lie somewhere in between these two cases. The third approximation, in fact, does lie between these two extremes and is constructed to give approximately the correct hierarchical amplitudes in the quasi-linear regime.

In the next section, we present the motivation for our three approximations and derive the form of the density PDF for local Lagrangian mappings. In Section 3, we use our approximations to derive analytic perturbative results in the quasi-linear regime for the evolution of both Gaussian and non-Gaussian initial conditions, and we discuss the effects of smoothing. In Section 4, we use our approximations in the nonlinear regime to derive the evolved PDF for Gaussian initial conditions, which we compare with numerical simulations. We then apply our approximations to a variety of non-Gaussian initial conditions. Our results and conclusions are summarized in Section 5. In the Appendix, we derive the relation between any local Lagrangian mapping of an initially Gaussian density field and the corresponding vertex generating function.

2 LOCAL LAGRANGIAN APPROXIMATIONS

To obtain the form of the evolved density PDF one has to use some approximation scheme describing the particle dynamics, as well as to adopt a set of initial conditions on the density field. One of the most efficient approximation schemes is the Zel'dovich approximation (ZA) (Zel'dovich 1970) which can be thought of as an operator acting on the initial (Lagrangian) comoving position $\mathbf{q}$ of a particle and yielding its final (Eulerian) comoving position $\mathbf{x}$. Specifically, one has:

$$\mathbf{x}(\mathbf{q},t) = \mathbf{q} + D(t)\mathbf{\Psi}(\mathbf{q}), \tag{3}$$

where $D(t)$ is a universal time dependent function proportional to the expansion factor $a(t)$ for a flat, pressureless universe, and $\mathbf{\Psi}(\mathbf{q})$ is proportional to the gradient of the initial gravitational potential.

The evolution of the PDF of the density field in the Zel'dovich approximation has been discussed in detail by Kofman et al. (1994); here we briefly summarize their results relevant to our work. Consider a particle of mass dm uniformly spread at time t_0 inside an infinitesimal Lagrangian volume d^3q. At some later time t the respective volume has evolved to the

Eulerian infinitesimal one d^3x_q. Mass conservation implies:

$$\rho(\mathbf{q},t)d^3x_q = \rho(\mathbf{q},t_0)d^3q, \tag{4}$$

In the quasi-linear regime prior to shell-crossing, multi-streaming may be neglected; here we make the assumption that multi-streaming is unimportant.

From equation (4) one obtains:

$$\rho(\mathbf{q},t) = \bar{\rho}\|\frac{\partial \mathbf{x}}{\partial \mathbf{q}}\|^{-1}, \tag{5}$$

According to equation (3) one has then:

$$\|\frac{\partial \mathbf{x}}{\partial \mathbf{q}}\|^{-1} = \|I + D\frac{\partial \mathbf{\Psi}}{\partial \mathbf{q}}\|^{-1}. \tag{6}$$

Taking $\eta \equiv \rho/\bar{\rho}$, equation (2.3) yields:

$$\eta = \frac{1}{\|1 - D\frac{\partial \mathbf{\Psi}}{\partial \mathbf{q}}\|}. \tag{7}$$

If $\partial\Psi_i/\partial q_j$ has eigenvalues λ_1, λ_2, and λ_3, then the expression for the evolved density in the Zel'dovich approximation can be written as:

$$\eta(\mathbf{q},t) = \frac{\eta_0(\mathbf{q})}{[1 - D(t)\lambda_1][1 - D(t)\lambda_2][1 - D(t)\lambda_3]}. \tag{8}$$

The distribution of λ can be calculated exactly in the case of Gaussian initial conditions, and the results applied to determine the exact form for $P(\rho)$ (Kofman et al. 1994). Unfortunately, the exact distribution of the eigenvalues of $\partial\Psi_i/\partial q_j$ is not easy to derive for most non-Gaussian models, so we consider several possible ways to simplify eq. (8).

We look for approximations to equation (8) which are "local", i.e., the right hand side is a function only of $D(t)$ and δ_0. To derive approximations of this sort, we note that the relation between δ_0 and the $\lambda' s$ is

$$\delta_0 = \lambda_1 + \lambda_2 + \lambda_3 \tag{9}$$

Consider first the approximation:

$$\eta(\mathbf{q},t) = \frac{\eta_0(\mathbf{q})}{[1 - D(t)(\lambda_1 + \lambda_2 + \lambda_3)]}. \tag{10}$$

With equation (9), this reduces to

$$\eta(\mathbf{q},t) = \frac{\eta_0(\mathbf{q})}{[1 - D(t)\delta_0(\mathbf{q})]}. \tag{11}$$

This approximation is exact in the limit of 1-dimensional collapse ($\lambda_2 = \lambda_3 = 0$) and corresponds to exact gravitational evolution in one dimension (Shandarin & Zel'dovich 1989).

Hence the results we derive for this approximation will give the exact evolution of the PDF in one dimension. Equation (11) has also been investigated as an approximation to the evolution of the density field in three dimensions (Nusser et al. 1991; Mataresse et al. 1992). We will refer to equation (11) as the *planar* approximation.

The other extreme case is spherical collapse, for which $\lambda_1 = \lambda_2 = \lambda_3$. In this case, equation (8) becomes

$$\eta(\mathbf{q}, t) = \frac{\eta_0(\mathbf{q})}{[1 - D(t)\delta_0(\mathbf{q})/3]^3}. \tag{12}$$

Equation (12) corresponds to the approximation of Padmanabhan and Subramanian (1993) in the limit of zero smoothing; this approximation was also used by Betancort-Rijo (1991) in a study of the evolution of the rms density fluctuation. We shall refer to this as the *spherical* approximation.

We expect that the actual evolution of the density field lies somewhere in between spherical and planar collapse. Note that both equations (11) and (12) are of the form

$$\eta(\mathbf{q}, t) = \frac{\eta_0(\mathbf{q})}{(1 - D(t)\delta_0(\mathbf{q})/\alpha)^\alpha}, \tag{13}$$

with $\alpha = 1$ for the planar approximation and $\alpha = 3$ for the spherical approximation. For our third approximation, we choose $\alpha = 3/2$ to obtain:

$$\eta(\mathbf{q}, t) = \frac{\eta_0(\mathbf{q})}{[1 - 2D(t)\delta_0(\mathbf{q})/3]^{3/2}}. \tag{14}$$

The choice of $\alpha = 3/2$ has no particular physical significance, but we show in the next section [based on earlier results of Bernardeau (1992) and Bernardeau & Kofman (1995)] that the hierarichal amplitudes for this model closely mimic the results of exact perturbation theory. For that reason, we will refer to equation (14) by the oxymoronic name of the *exact* approximation.

How do we get from the Lagrangian mappings given by equations (11), (12), and (14) to the evolved density distribution function? Following Kofman et al. (1994), we define $P(\rho)$ (or, equivalently, $P(\eta)$) to be the Eulerian density distribution function and take $Q(\rho)$ to be the Lagrangian distribution function. Basically, $P(\rho)$ gives the probability that a randomly-selected point in space has a density in the interval ρ to $\rho + d\rho$, while $Q(\rho)$ is the probability that a randomly-selected mass point has a density in that interval. Since the probability of "randomly" selecting a given mass point at an Eulerian location $\mathbf{x}$ is proportional to the density at $\mathbf{x}$, we have (Kofman et al. 1994) $Q(\rho) = (\rho/\bar{\rho})P(\rho)$, or

$$P(\eta) = \frac{1}{\eta} Q(\eta). \tag{15}$$

Furthermore, we assume an initial Eulerian distribution $P_0(\eta_0)$ and initial Lagrangian distribution $Q_0(\eta_0)$, also related by $P_0(\eta_0) = Q_0(\eta_0)/\eta_0$. Given a Lagrangian mapping of the form $\eta(\mathbf{q}, t) = f(\eta_0(\mathbf{q}), t)$, the evolved Lagrangian PDF is

$$Q(\eta) = Q_0(f^{-1}(\eta)) \frac{df^{-1}(\eta)}{d\eta}, \tag{16}$$

where f^{-1} is the inverse of the Lagrangian mapping given in equation (1). Using the relations between the Lagrangian and Eulerian distributions functions, we can express the final Eulerian density distribution in terms of the initial Eulerian distribution:

$$P(\eta) = P_0(f^{-1}(\eta))\frac{f^{-1}(\eta)}{\eta}\frac{df^{-1}(\eta)}{d\eta}. \tag{17}$$

All of these equations can be simplified by taking our initial epoch sufficiently early that $\eta_0 \approx 1$ and $P_0(\eta_0) \approx Q_0(\eta_0)$. In particular, equation (17) becomes

$$P(\eta) = P_0(f^{-1}(\eta))\frac{1}{\eta}\frac{df^{-1}(\eta)}{d\eta}. \tag{18}$$

Note that in order for P and Q to represent probability distribution functions, they must satisfy

$$\int Q(\eta)d\eta = 1, \tag{19}$$

and

$$\int P(\eta)d\eta = 1. \tag{20}$$

Equation (19) is equivalent to mass conservation and is automatically satisfied by local Lagrangian mappings of the form given in equation (1). Equation (20) gives the conservation of Eulerian volume, and it is not automatically satisfied. Assuming that our initial distribution functions P_0 and Q_0 are correctly normalized, then equation (20) is satisfied by the Zel'dovich approximation and our planar approximation; it is not satisfied by equation (13) for $\alpha \neq 1$, and therefore the spherical and exact approximations fail this test. Hence, we cannot use equations (12) or (14) as written as valid approximations for the evolution of the density. To correct this problem, we modify equation (1) to read

$$\eta(\mathbf{q}, t) = N(t)f(\eta_0(\mathbf{q}), t), \tag{21}$$

where $N(t)$ is a time-dependent function given by substituting equation (18) into our normalization condition [equation (20)]:

$$N(t) = \int \frac{1}{f(\eta_0, t)}P_0(\eta_0)d\eta_0 = \langle\frac{1}{f(\eta_0, t)}\rangle \tag{22}$$

With the correct normalization, our general mapping given by eq. (13) becomes

$$\eta(\mathbf{q}, t) = \frac{\langle(1 - D(t)\delta_0(\mathbf{q})/\alpha)^\alpha\rangle}{(1 - D(t)\delta_0(\mathbf{q})/\alpha)^\alpha}. \tag{23}$$

Note that our $N(t)$ resembles the multistreaming factor N_s discussed in Kofman et al. (1994), although our factor has been introduced as a mathematical construct in order to keep our probabilities normalized.

3 PERTURBATIVE RESULTS

3.1 Gaussian Initial Conditions

In order to test our mappings for agreement with the true gravitational evolution of the PDF, we will first consider the quasilinear case $|\delta(t)| \lesssim 1$. In this limit a number of perturbative results are known for the evolution of Gaussian initial conditions, and a few for non-Gaussian initial conditions, which can be compared with the perturbative predictions of our local Lagrangian approximations.

The density field can be described in terms of the cumulants κ_p, which are functions of the moments of the density field $\langle \delta^p \rangle$. The first few cumulants are given by (see Stuart & Ord 1987 for a more detailed discussion)

$$\begin{aligned} \kappa_2 &= \langle \delta^2 \rangle \\ \kappa_3 &= \langle \delta^3 \rangle \\ \kappa_4 &= \langle \delta^4 \rangle - 3\langle \delta^2 \rangle^2 \end{aligned} \tag{24}$$

For Gaussian initial conditions, it is possible to show that the cumulants κ_p of the evolved density field satisfy $\kappa_p/\sigma^{2(p-1)} \rightarrow$ constant in the limit $\sigma \rightarrow 0$, where $\sigma = \langle \delta^2 \rangle^{1/2}$, and the constants are called the hierarchical amplitudes, denoted S_p:

$$S_p = \kappa_p/\sigma^{2(p-1)} \tag{25}$$

This result was first derived for the skewness (κ_3) by Peebles (1980), for the kurtosis (κ_4) by Fry (1984), and a method for calculating the full hierarchy of the S_p was derived by Bernardeau (1992). Our local Lagrangian approximations also produce a hierarchical clustering pattern (i.e., the cumulants of the evolved distribution satisfy equation 25). Of course, there is little point in using approximations to derive S_p in the Gaussian case, since these values can be calculated exactly. However, it is precisely because the S_p's are known exactly that the calculation of S_p for the Gaussian case can be used to estimate the accuracy and general behavior of our approximations. This calculation also serves as a warm-up for the case of non-Gaussian initial conditions, for which no general results for S_p have been derived (although see Fry & Scherrer 1994; Chodorowski & Bouchet 1996).

First note that all of our mappings (equations 11, 12, 14) can be expressed in the form

$$\eta(\mathbf{q}, t) = f[\delta_l(\mathbf{q})], \tag{26}$$

where δ_l is the linearly-evolved density: $\delta_l(\mathbf{q}) \equiv D(t)\delta_0(\mathbf{q})$. Consider first the planar mapping given by equation (11). Taking $\eta_0(\mathbf{q}) = 1$ we obtain:

$$\eta(\mathbf{q}, t) = 1 + \delta_l(\mathbf{q}) + \delta_l(\mathbf{q})^2 + \delta_l(\mathbf{q})^3 + ... \tag{27}$$

To calculate S_3, we need to find $\kappa_3 = \langle \delta^3 \rangle_E$, where we now distinguish between Eulerian averages (effectively taken over volume and denoted with a subscript E) and Lagrangian averages (taken over mass and denoted with a subscript L). Our task is to express the Eulerian average of powers of δ [which are the numbers which enter into equation (24)] in terms of the Lagrangian average of powers of η [which can be derived from equation (27)]. For powers of η, the relation between the Eulerian and Lagrangian averages takes the simple form

$$\langle \eta^n \rangle_E = \langle \eta^{n-1} \rangle_L \tag{28}$$

which follows directly from equation (15). Then we can express κ_3 as

$$\begin{aligned} \kappa_3 &= \langle (\eta - 1)^3 \rangle_E \\ &= \langle \eta^2 \rangle_L - 3\langle \eta \rangle_L + 2 \end{aligned} \tag{29}$$

Combining equation (29) with equation (27), we obtain, for the planar approximation,

$$\kappa_3 = \sum_{j=1}^{\infty} \langle (j-2)\delta_l^j \rangle. \tag{30}$$

For Gaussian initial conditions,

$$\begin{aligned} \langle \delta_l^j \rangle &= (j-1)!!\sigma^j \quad (j \text{ even}), \\ &= 0 \quad (j \text{ odd}), \end{aligned} \tag{31}$$

where $\sigma_l \equiv \langle \delta_l^2 \rangle^{1/2} = D(t)\sigma_0$ is the linearly-evolved rms fluctuation. Then we end up with

$$\kappa_3 = \sum_{n=2}^{\infty} 2(n-1)(2n-1)!!\sigma_l^{2n}, \tag{32}$$

so that

$$S_3(\sigma_l) = \sum_{n=2}^{\infty} 2(n-1)(2n-1)!!\sigma_l^{2n-4} = 6 + 60\sigma_l^2 + O(\sigma_l^4), \tag{33}$$

and $S_3(0) = 6$. This result has been derived previously by Bernardeau & Kofman (1995) using more complex techniques, but our σ^2 term differs from theirs. At this point, we must be careful about our definition of the hierarchical amplitudes. In equation (25), we have used the *linearly-evolved* rms fluctuation σ_l, rather than the true rms fluctuation $\sigma = \langle \delta^2 \rangle^{1/2}$. If instead we use the true rms fluctuation, we can define a new set of hierarchical amplitudes, given by:

$$\widetilde{S}_p(\sigma) = \kappa_p / \langle \delta^2 \rangle^{p-1} \tag{34}$$

This distinction is usually ignored, because $S_p(0) = \widetilde{S}_p(0)$ for Gaussian initial conditions. However, when expanding S_p to higher order, or when dealing with non-Gaussian initial conditions (Fry & Scherrer 1994), the distinction must be made. Note that $\widetilde{S}_p$ is closer to what observers actually measure. When we expand $\langle \delta^2 \rangle_E = \langle \eta \rangle_L - 1$, we obtain

$$\sigma^2 = \sigma_l^2 + 3\sigma_l^4 + O(\sigma_l^6). \tag{35}$$

Substituting this into equation (34) and reexpressing everything in terms of σ rather than σ_l, we obtain an expression for $\widetilde{S}_p$ which agrees with Bernardeau & Kofman:

$$\widetilde{S}_3(\sigma) = 6 + 24\sigma^2 + O(\sigma^4) \tag{36}$$

Note that because $\sigma^2 = \sigma_l^2 + O(\sigma_l^4)$, it does not matter if we use σ_l or σ on the right-hand side of equation (36), although it would make a difference if we expanded out to fourth order in σ.

We can similarly expand the expression for κ_4 to obtain

$$\kappa_4 = \langle \eta^3 \rangle_L - 4\langle \eta^2 \rangle_L - 3\langle \eta \rangle_L^2 + 12\langle \eta \rangle_L - 6 \tag{37}$$

Again, substituting equation (27) for η in equation (37), expanding out term by term, and taking the averages appropriate to the Gaussian initial conditions from equation (31), we obtain $S_4(0) = 72$, in agreement with Bernardeau & Kofman (1995).

Now consider the spherical approximation (equation 12). This approximation is complicated by the fact that for Gaussian initial conditions, $\langle 1/f(\eta_0,t)\rangle \neq 1$, so we have to include the normalizing factor given by equation (22). For Gaussian initial conditions, the normalizing factor in equation (22) for the spherical approximation is

$$N = \langle (1 - D(t)\delta_0/3)^3 \rangle = 1 + \sigma_l^2/3 \tag{38}$$

and the spherical mapping becomes:

$$\eta(\mathbf{q},t) = \frac{1+\sigma_l^2/3}{(1-\delta_l/3)^3}. \tag{39}$$

Substituting this mapping into equations (29) and (37) and taking the appropriate averages for the Gaussian initial distribution from equation (31) we obtain

$$S_3(0) = 4 \tag{40}$$
$$S_4(0) = 272/9 \tag{41}$$

Oddly, these are identical to the hierarchical amplitudes obtained for the full Zel'dovich approximation (see, for example, Munshi et al. 1994; Bernardeau & Kofman 1995). In fact, we can show that the spherical approximation and the Zeldovich approximation have identical values for *all* of the hierarchical amplitudes $S_p(0)$. To do this, we introduce the vertex generating function for the density field (Bernardeau 1992)

$$G_\delta(\tau) = \sum_{n=1}^{\infty} \frac{\nu_n}{n!}\tau^n, \tag{42}$$

where

$$\nu_n = \frac{\int \langle \delta^{(n)}(\mathbf{x})\delta^{(1)}(\mathbf{x}_1)...\delta^{(1)}(\mathbf{x}_n)\rangle_c d^3\mathbf{x}\; d^3\mathbf{x}_1...d^3\mathbf{x}_n}{(\int \langle \delta^{(1)}(\mathbf{x})\delta^{(1)}(\mathbf{x}')\rangle d^3\mathbf{x}\; d^3\mathbf{x}')^n}, \tag{43}$$

and $\delta^{(n)}$ is the n_{th}-order expansion of δ. [Our convention for the sign of τ is the same as that of Munshi et al. (1994) and the opposite of Bernardeau (1992) and Bernardeau & Kofman (1995)]. The values of the ν_n totally determine $S_p(0)$, through the relations:

$$S_3(0) = 3\nu_2,$$
$$S_4(0) = 4\nu_3 + 12\nu_2^2, \tag{44}$$

and so on (Bernardeau 1992).

In the Appendix, we demonstrate an extremely useful result for local Lagrangian mappings with Gaussian initial conditions: for a given mapping $\eta(\mathbf{q},t) = N(t)f[\delta_l(\mathbf{q})]$, where δ_l is the linearly-evolved density, the vertex generation function is just given by the same Lagrangian mapping without the normalizing function:

$$G_\delta(\tau) = f(\tau) - 1 \tag{45}$$

[In fact, the same result holds for local Eulerian mappings, but these are not the subject of this paper]. For the spherical approximation, equation (45) gives

$$G_\delta(\tau) = \frac{1}{(1-\tau/3)^3} - 1 \tag{46}$$

which is identical to $G_\delta(\tau)$ for the Zeldovich approximation (Munshi, et al.). Thus, $S_p(0)$ for our spherical approximation and $S_p(0)$ for the Zeldovich approximation will be identical for all p. This does not mean that the spherical approximation and the Zeldovich approximation produce identical evolved PDF's. The reason is that although $S_p(0)$ is the same for these two approximations, the $S_p(\sigma)'s$ differ at higher order in σ. The importance of considering higher-order σ terms has been emphasized by Bernardeau & Kofman (1995), and Scoccimarro & Frieman (1996) have recently calculated the higher-order corrections for the Zeldovich approximation. Scoccimarro & Frieman obtain, for $S_3(\sigma)$:

$$S_3(\sigma_l) = 4 + (1112/75)\sigma_l^2 + O(\sigma_l^4) \quad (47)$$

$$\widetilde{S}_3(\sigma) = 4 + (352/75)\sigma^2 + O(\sigma^4) \quad (48)$$

In comparison, our spherical approximation gives:

$$S_3(\sigma_l) = 4 + (286/27)\sigma_l^2 + O(\sigma_l^4) \quad (49)$$

$$\widetilde{S}_3(\sigma) = 4 + (118/27)\sigma^2 + O(\sigma^4). \quad (50)$$

Although the higher-order contributions to S_3 are of similar magnitude in the two cases, they are not identically equal, so the spherical approximation and Zeldovich approximation give different density distributions. This result demonstrates the importance of higher-order calculations: two density fields can have identical $S_p(0)$ for all p and yet have different PDF's.

The result given in equation (45) leads naturally to our "exact" approximation (equation 14). An expression for $G_\delta(\tau)$ can be calculated in parametric form for the case of the exact evolution of the density field (Bernardeau 1992; Munshi et al. 1994; Bernardeau & Kofman 1995):

$$G_\delta(\tau) = \frac{9}{2}\frac{(\theta - \sin\theta)^2}{(1-\cos\theta)^3} - 1,$$

$$\tau = \frac{3}{5}[\frac{3}{4}(\theta - \sin\theta)]^{2/3}, \quad (51)$$

for $\tau > 0$, and

$$G_\delta(\tau) = \frac{9}{2}\frac{(\sinh\theta - \theta)^2}{(\cosh\theta - 1)^3} - 1,$$

$$\tau = -\frac{3}{5}[\frac{3}{4}(\sinh\theta - \theta)]^{2/3}, \quad (52)$$

for $\tau < 0$. Bernardeau (1992) and Bernardeau & Kofman (1995) have noted that an excellent approximation for $G_\delta(\tau)$ for the case of exact evolution is given by

$$G_\delta(\tau) = (1 - 2\tau/3)^{-3/2} - 1. \quad (53)$$

Now we can argue backwards from our result in equation (45): the local Lagrangian mapping

$$\eta(\mathbf{q}, t) = \frac{\langle(1 - 2\delta_l/3)^{3/2}\rangle}{(1 - 2\delta_l/3)^{3/2}} \quad (54)$$

will produce a hierarchy of $S_p(0)$ very close to the results of exact evolution. Hence, the local Lagrangian mapping given in equation (54) should provide a good approximation to the true evolution in the quasi-linear regime. As expected, the lowest order hierarchical amplitudes for this approximation are in excellent agreement with the exact values: our approximation gives $S_3(0) = 5$, $S_4(0) = 440/9 \approx 48.9$, compared to $S_3(0) = 4.9$ and $S_4(0) = 45.9$ for the exact quasi-linear evolution.

We note in passing that using equations (51)-(52), along with equation (45), it is possible to derive a local Lagrangian approximation in parametric form which *exactly* reproduces the hierarchical amplitudes $S_p(0)$ for all p. However, the extra complexity involved in the parametric representation, plus the fact that higher order terms will diverge from their correct values anyway, probably makes this approximation less useful than our "exact" approximation.

Now let us evaluate the usefulness of the approximations which we have derived. A comparison of $G_\delta(\tau)$ for the planar and spherical approximations with $G_\delta(\tau)$ for the case of exact evolution, expanded out in a power series (Munshi et al. 1994) shows that the coefficients in the expansion for the planar case are larger than the corresponding coefficients for exact evolution, while the opposite is true for the spherical approximation. Thus, $S_p(0)$ for the planar approximation gives an upper bound on the true $S_p(0)$, while $S_p(0)$ for the spherical approximation gives a lower bound. In that sense, these two approximations bound the true evolution of the PDF: the planar approximation gives a PDF which deviates more strongly from a Gaussian than the true evolution, while the spherical approximation yields a PDF which deviates less from a Gaussian. This makes physical sense, since these two approximations correspond to planar collapse and spherical collapse, respectively, and the true evolution should lie somewhere in between. The "exact" approximation, on the other hand, should provide a reasonable approximation to the evolution of the PDF for quasi-linear evolution.

All of these calculations are valid only for Gaussian initial conditions. However, it is plausible that our three approximations can be extended to provide some insight into the evolution of the PDF for the case of non-Gaussian initial conditions: arguing in analogy with the Gaussian case, we expect the planar and spherical approximations to provide upper and lower bounds on the deviation of the PDF from the initial conditions, while the "exact" approximation should give a good estimate of the overall evolution. More importantly, any features in the evolution shared by all three approximations are likely to be true characteristics of the gravitational evolution of the PDF.

3.2 Effects of Smoothing

Before venturing into the murky world of non-Gaussian initial conditions, we must consider the effects of smoothing. Our approximations and results in the previous section apply only to the unsmoothed density field, while it is the smoothed density field which is actually observed. Since our local Lagrangian approximations give only the PDF and do not provide a prescription for actually moving the matter around, there is in principle no way to derive smoothed versions of them. However, we can derive plausible "smoothed" approximations which give the same hierarchical amplitudes as the smoothed mappings would.

Our argument is based on the calculations of Bernardeau (1994), who showed that for a spherical tophat window function, there is a simple relation between $G_\delta(\tau)$ for a particular density field, and $G^S_\delta(\tau)$ for the corresponding smoothed density field. For simplicity, we consider only a density field with a power-law power spectrum $P(k) \propto k^n$, for which Bernardeau (1994) obtained the implicit equation

$$G^S_\delta(\tau) = G_\delta(\tau[1 + G^S_\delta(\tau)]^{-(n+3)/6}). \tag{55}$$

Consider the vertex function of the density field produced by first applying a given local Lagrangian mapping, and then smoothing. Using equation (55), we can generate a "smoothed" local Lagrangian mapping which produces a final density field with the same vertex generating function. To do this, we simply use equation (45): for local Lagrangian approximations, a transformation of the vertex generating function corresponds to the same transformation of the Lagrangian mapping. Thus, for a given mapping $\eta(\mathbf{q},t) = N(t)f(\delta_l)$, the "smoothed" mapping is given by

$$\eta_S = f^S(\delta_l) = f(\delta_l[f_S(\delta_l)]^{-(n+3)/6}) \tag{56}$$

where $f^S(\delta_l)$ must then be multiplied by the normalizing factor specified by equation (20). Note that this does *not* mean that $f^S(\delta_l)$ corresponds to the density field derived by applying the mapping $\eta = f(\delta_l)$ and then smoothing; rather, $f_S(\delta_l)$ will produce a density field with the same hierarchical amplitudes $S_p(0)$ as the field derived by first applying $f(\delta_l)$ and then smoothing. Hence, we expect $f^S(\delta_l)$ given by equation (56) to provide a good approximation to the PDF of the smoothed density field.

We will confine our attention to the case $n = -1$, because it corresponds roughly to the the slope of the CDM power spectrum on galaxy clustering scales, and this choice allows us to compare with previous work. For the spherical and "exact" approximations, this case produces particularly simple smoothed mappings. For the spherical mapping, equation (56) applied to the mapping given by equation (12) gives (Bernardeau & Kofman 1995)

$$\eta_S = (1+\delta_l/3)^3\langle(1+\delta_l/3)^{-3}\rangle \tag{57}$$

while for the exact approximation, equations (56) and (14) yield (Bernardeau 1994):

$$\eta_S = (\delta_l/3+\sqrt{1+\delta_l^2/9})^3\langle(\delta_l/3+\sqrt{1+\delta_l^2/9})^{-3}\rangle \tag{58}$$

For the planar approximation, we obtain a cubic equation for η_S, which yields

$$\eta_S = [g^{1/3}+\delta_l^2/9g^{1/3}+\delta_l/3]^3\langle[g^{1/3}+\delta_l^2/9g^{1/3}+\delta_l/3]^{-3}\rangle, \tag{59}$$

where $g(\delta_l)$ is defined by

$$g = 1/2+\delta_l^3/27+(12\delta_l^3+81)^{1/2}/18. \tag{60}$$

We can now apply both the smoothed and unsmoothed approximations to the case of non-Gaussian initial conditions.

3.3 Non-Gaussian Initial Conditions

We now repeat our perturbative calculations from Section 3.1 for the case of non-Gaussian initial conditions. The methods are identical to those used in Section 3.1; the only difference is that for non-Gaussian initial conditions, all terms of the form $\langle\delta_l^p\rangle$ must be retained, rather than being reduced to various powers of σ as we did for Gaussian initial conditions (equation 31). This alters not just our final expression derived from our mappings, but also changes the normalization factor for each mapping.

Consider first the rms fluctuation $\langle\delta^2\rangle$. The most interesting question one can ask about $\langle\delta^2\rangle$ is whether the first correction gives growth which is faster or slower than linear. For Gaussian initial conditions, the first correction to linear theory is of order σ^4. This correction has recently been examined in detail by Lokas et al. (1996) and Scoccimarro & Frieman (1996); they find that for unsmoothed density fields,

$$\langle\delta^2\rangle = \sigma_l^2+1.8\sigma_l^4 \tag{61}$$

For smoothed initial conditions, the sign of the σ^4 term depends on the initial power index; it is negative for $n \geq -1$ but positive for $n = -2$.

As noted by Fry & Scherrer (1994), the first correction to $\langle\delta^2\rangle$ for non-Gaussian initial conditions is of order σ^3, rather than σ^4, suggesting that non-Gaussian initial conditions should give an earlier divergence from linear behavior. Fry & Scherrer (1994) found that for arbitrary initial conditions,

$$\langle\delta^2\rangle = \sigma_l^2 + \frac{13}{21}\langle\delta_l^3\rangle + \frac{4}{7}I[\zeta_0], \tag{62}$$

where $I[\zeta_0]$ is an integral over the initial three-point function of the non-Gaussian distribution. If the second term in equation (62) dominates the third term or has the same sign as the third term, then the sign of the initial skewness determines whether the rms density evolves more or less rapidly than linear, with positive skewness models evolving more rapidly and negative skewness models less rapidly. However, all of these results apply only to the unsmoothed density field.

Using our approximations from Section 2 and our perturbative methods from Section 3, we obtain, for the unsmoothed density field, the following expressions for $\langle\delta^2\rangle$:

$$\langle\delta^2\rangle = \sigma_l^2 + \langle\delta_l^3\rangle + \langle\delta_l^4\rangle + O(\sigma^5), \quad \text{(planar)}, \tag{63}$$

$$\langle\delta^2\rangle = \sigma_l^2 + \frac{2}{3}\langle\delta_l^3\rangle + \frac{53}{108}\langle\delta_l^4\rangle + \frac{5}{36}\sigma_l^4 + O(\sigma^5), \quad \text{(exact)}, \tag{64}$$

$$\langle\delta^2\rangle = \sigma_l^2 + \frac{1}{3}\langle\delta_l^3\rangle + \frac{5}{27}\langle\delta_l^4\rangle + \frac{2}{9}\sigma_l^4 + O(\sigma^5), \quad \text{(spherical)}. \tag{65}$$

For the Gaussian case, we see that the first correction term is $3\sigma^4$ for the planar case, $1.61\sigma^4$ for the exact approximation, and $0.78\sigma^4$ for the spherical approximation. Once more, we see that the planar and spherical cases bracket the exact perturbative result, while the exact approximation comes close to the exact perturbative value. For the non-Gaussian case, the expression for the exact evolution is non-local, as shown in equation (62). However, in the limit where the long-range correlations in the initial density field are small, equation (62) reduces to $\langle\delta^2\rangle = \langle\delta_l^2\rangle + (13/21)\langle\delta_l^3\rangle$. The nonlinear correction term in this case is nearly identical to the correction term in the exact approximation, $(2/3)\langle\delta_l^3\rangle$, and is again bracketed by the correction terms for the planar and spherical approximations. In all three of our approximations, the lowest-order nonlinear correction is a positive multiple of the initial skewness, so that positive-skewness models have larger rms densities and negative-skewness models have smaller rms densities than predicted by linear theory, in agreement with the conjecture of Fry & Scherrer (1994).

The simulations of Weinberg and Cole (1992) do not unambiguously support this conclusion for the case of smoothed density fields, so we consider what happens when we use our smoothed mappings from the previous section. Using the mappings for $n = -1$ derived in the previous section, we find:

$$\langle\delta^2\rangle = \sigma_l^2 + \frac{1}{3}\langle\delta_l^3\rangle + \frac{1}{9}\langle\delta_l^4\rangle + \frac{2}{9}\sigma_l^4 + O(\sigma^5), \quad \text{(planar)}, \tag{66}$$

$$\langle\delta^2\rangle = \sigma_l^2 + \frac{5}{108}\langle\delta_l^4\rangle + \frac{1}{4}\sigma_l^4 + O(\sigma^5), \quad \text{(exact)}, \tag{67}$$

$$\langle\delta^2\rangle = \sigma_l^2 - \frac{1}{3}\langle\delta_l^3\rangle + \frac{5}{27}\langle\delta_l^4\rangle + \frac{2}{9}\sigma_l^4 + O(\sigma^5), \quad \text{(spherical)}. \tag{68}$$

We see that the effect of smoothing for $n = -1$ is to significantly reduce the growth of $\langle\delta^2\rangle$ as compared with the unsmoothed case. In particular, we can draw no unambiguous conclusions regarding the dependence of $\langle\delta^2\rangle$ on the sign of the skewness; our three approximations give different answers, and in our exact approximation, there is no skewness dependence at all.

Now consider the evolution of the skewness itself. As noted in section 3.1, we must distinguish between $S_3(\sigma) = \kappa_3/\langle\delta_l^2\rangle^4$ and $\widetilde{S}_3(\sigma) = \kappa_3/\langle\delta^2\rangle^4$. For non-Gaussian initial conditions these two quantities are not equal even in the limit $\sigma \to 0$, because of the terms containing $\langle\delta_l^3\rangle$ in the expansion for $\langle\delta^2\rangle$. Here we will consider only $\tilde{S}_3(0)$, because this is the quantity measured by observers; it is also the definition of skewness used by Fry & Scherrer (1994). Again, using the mappings in Sections 2 and 3.2 along with the expression for $\tilde{S}_3$ in section 3.1, we can obtain expressions for $S_3(0)$ for our various approximations. For comparison with the Gaussian case (and with previous work) it is convenient to express these results in terms of the linearly-evolved kurtosis, defined by $\kappa_{4l} \equiv= \langle\delta_l^4\rangle - 3\sigma_l^4$, which vanishes for Gaussian initial conditions. For the unsmoothed case, we obtain:

$$\widetilde{S}_3(0) = \frac{\langle\delta_l^3\rangle}{\sigma_l^4} + 6 + 2\frac{\kappa_{4l}}{\sigma_l^4} - 2\frac{\langle\delta_l^3\rangle^2}{\sigma_l^6}, \quad \text{(planar)} \tag{69}$$

$$\widetilde{S}_3(0) = \frac{\langle\delta_l^3\rangle}{\sigma_l^4} + 5 + \frac{3}{2}\frac{\kappa_{4l}}{\sigma_l^4} - \frac{4}{3}\frac{\langle\delta_l^3\rangle^2}{\sigma_l^6}, \quad \text{(exact)} \tag{70}$$

$$\widetilde{S}_3(0) = \frac{\langle\delta_l^3\rangle}{\sigma_l^4} + 4 + \frac{\kappa_{4l}}{\sigma_l^4} - \frac{2}{3}\frac{\langle\delta_l^3\rangle^2}{\sigma_l^6}, \quad \text{(spherical)}. \tag{71}$$

The exact perturbative result for $\widetilde{S}_3(0)$ for non-Gaussian initial conditions (Fry & Scherrer 1994) contains non-local terms involving integrals over the the initial three- and four-point functions. However, in the limit where these terms are small (e.g., for the case of weak correlations in the initial density field), the exact perturbative result is:

$$\widetilde{S}_3(0) = \frac{\langle\delta_l^3\rangle}{\sigma_l^4} + \frac{34}{7} + \frac{10}{7}\frac{\kappa_{4l}}{\sigma_l^4} - \frac{26}{21}\frac{\langle\delta_l^3\rangle^2}{\sigma_l^6}, \quad \text{(exact)}. \tag{72}$$

This expression is remarkably close to our result for the "exact approximation", and it is bracketed by the results for the planar and spherical approximations.

For the smoothed case, we obtain the results:

$$\widetilde{S}_3(0) = \frac{\langle\delta_l^3\rangle}{\sigma_l^4} + 4 + \frac{\kappa_{4l}}{\sigma_l^4} - \frac{2}{3}\frac{\langle\delta_l^3\rangle^2}{\sigma_l^6}, \quad \text{(planar)} \tag{73}$$

$$\widetilde{S}_3(0) = \frac{\langle\delta_l^3\rangle}{\sigma_l^4} + 3 + \frac{1}{2}\frac{\kappa_{4l}}{\sigma_l^4}, \quad \text{(exact)} \tag{74}$$

$$\widetilde{S}_3(0) = \frac{\langle\delta_l^3\rangle}{\sigma_l^4} + 2 + \frac{2}{3}\frac{\langle\delta_l^3\rangle^2}{\sigma_l^6}, \quad \text{(spherical)}. \tag{75}$$

There are no exact perturbative results with which we can compare our smoothed expressions for $\widetilde{S}_3$, but they display qualitatively the correct behavior; the effect of smoothing is to reduce the evolved skewness.

The results of this section for non-Gaussian initial conditions confirm the conclusions we reached in Section 3.1. Our "exact" approximation for the unsmoothed case agrees well

with perturbative results for non-Gaussian initial conditions, while the planar and spherical results bracket the known perturbative results. This suggests that our "exact" approximation should give reasonable results when we go on to calculate the full evolved PDF for a variety of non-Gaussian initial conditions, while the planar and spherical approximations may serve as useful bounds on the evolution. The situation is murkier with regard to our smoothed approximations, but they show at least qualitatively the correct behavior.

4 THE EVOLVED PDF

We can now apply our local Lagrangian mappings to derive the evolved PDF for any set of initial conditions using equation (18). Since we no longer assume $\delta_l \ll 1$, we have to modify our generic mapping given in eq. (23). Following Kofman et al. (1994) we take

$$\eta(\mathbf{q},t) = \frac{N(t)}{|1-\delta_l/\alpha|^\alpha} \tag{76}$$

where the normalization factor $N(t)$ is now given by

$$N(t) = \langle |1-\delta_l/\alpha|^\alpha \rangle \tag{77}$$

and the average is taken over the distribution of δ_l.

Consider first the case of Gaussian initial conditions. Then for the unsmoothed case, equation (18) gives

$$P(\eta)d\eta = \frac{1}{\sqrt{2\pi}\sigma_l}(\frac{\eta}{N})^{-1/\alpha-2}\Big[e^{-\alpha^2[1-(\eta/N)^{-1/\alpha}]^2/2\sigma_l^2} + e^{-\alpha^2[1+(\eta/N)^{-1/\alpha})]^2/2\sigma_l^2}\Big]\frac{d\eta}{N^2}, \tag{78}$$

where N is given by

$$N = \int_{-\infty}^{\infty}\frac{1}{\sqrt{2\pi}\sigma_l}e^{-\delta_l^2/2\sigma_l^2}|1-\frac{\delta_l}{\alpha}|^\alpha d\delta_l. \tag{79}$$

Note that this expression for $P(\eta)$ bears some resemblence to the distribution function derived by Bernardeau (1994), [eq. (19)], using more sophisticated techniques, but the two distributions are different.

For our smoothed mappings, the results are even simpler. If we assume a mapping of the form in equation (76) smoothed with a spherical tophat window function, with a k^n power spectrum, we obtain from equation (56) the following relation between the evolved value for η and the linear perturbation δ_l:

$$\delta_l = \alpha\Big[(\frac{\eta}{N})^{(n+3)/6} - (\frac{\eta}{N})^{-1/\alpha+(n+3)/6}\Big], \tag{80}$$

which can be substituted into the Gaussian expression for δ_l, with the appropriate normalizing factor, to obtain $P(\eta)$. For example, for $n=-1$ we obtain

$$P(\eta)d\eta = \frac{1}{\sqrt{2\pi}\sigma_l}\alpha[(\frac{1}{3}(\frac{\eta}{N})^{-5/3}+(\frac{1}{\alpha}-\frac{1}{3})(\frac{\eta}{N})^{-1/\alpha-5/3}]\exp\Big(-\alpha^2[(\frac{\eta}{N})^{1/3}-(\frac{\eta}{N})^{1/3-1/\alpha}]^2/2\sigma_l^2\Big)\frac{d\eta}{N^2} \tag{81}$$

For the "exact" approximation ($\alpha = 3/2$), this reduces to

$$P(\eta)d\eta = \frac{1}{2\sqrt{2\pi}\sigma_l}[(\frac{\eta}{N})^{-5/3} + (\frac{\eta}{N})^{-7/3}]\exp\Big(-\frac{9}{8\sigma_l^2}[(\frac{\eta}{N})^{1/3} - (\frac{\eta}{N})^{-1/3}]^2\Big)\frac{d\eta}{N^2}, \tag{82}$$

where N in this case is given by

$$N = \int_{-\infty}^{\infty} \frac{1}{\sqrt{2\pi}\sigma_l} e^{-\delta_l^2/2\sigma_l^2} \left[\frac{1}{3}\delta_l + \sqrt{1+\frac{\delta_l^2}{9}}\right]^{-3} d\delta_l \tag{83}$$

We can compare these results with numerical simulations of gravitational clustering. We have used the simulations of Weinberg (Juszkiewicz et al. 1995; Lokas et al. 1995) with power-law initial conditions, smoothed with a spherical tophat. In Figure 1, we show the case $n = -1$, for $\sigma_l = 0.5$, 0.75, and 1. The points are the results of averaging eight numerical simulations with 1-σ error bars, and the solid curve is the smoothed "exact" approximation, equation (82). For $\sigma_l = 0.5$, the agreement is remarkable, particularly given the simplicity of the approximation which led to equation (82). There is still reasonable agreement at $\sigma_l = 0.75$, but the approximation begins to break down at this point, and agreement is poor for $\sigma_l = 1.0$. These results are not surprising, since the "exact" approximation was designed to mimic the exact hierarchical amplitudes in the limit where $\sigma_l \to 0$, and it can be expected to break down when the contributions to S_p of higher order in σ_l become important. In fact, Scoccimarro & Frieman (1996) have argued that this should occur at $\sigma_l^2 \sim 1/2$, which is precisely when our approximation appears to break down in Fig. 1. In Fig. 2, we show the planar and spherical approximations along with the numerical simulations for $\sigma_l = 0.5$ and $\sigma_l = 0.75$. For $\sigma_l = 0.5$, the planar and spherical approximations do indeed bound the numerical results, but the spherical approximation breaks down completely at $\sigma_l = 0.75$. In fact, it is easy to show from equation (81) that the spherical approximation breaks down (in the sense of no longer having central maximum near $\eta = 1$) at $\sigma_l^2 = 9/20$. Again, this is near the point at which Scoccimarro and Frieman (1996) predict a breakdown of perturbation theory.

The importance of using our smoothing method derived from Bernardeau (1994) is illustrated in Fig. 3. There we show, for $\sigma_l = 0.5$, all three of our approximations for the unsmoothed PDF. All three of them differ strongly from the numerical results, showing greater deviation from the original Gaussian. This is not surprising, since these approximations are only appropriate for the PDF measured for an unsmoothed density field, or for a smoothed density field with initial power spectrum $P(k) \propto k^{-3}$.

Finally, we note that our results in the Appendix indicate that there is also a local Eulerian mapping which has a vertex generating function equal to $G_\delta(\tau) = 1/(1-2\tau/3)^{3/2}$ and which should therefore also give an excellent approximation to the evolved PDF in the quasilinear regime. This Eulerian approximation is given by taking $\eta(\mathbf{x},t) = f[\delta_l(\mathbf{x})]$, with the mapping given by equation (76) or (80) for the unsmoothed and smoothed density fields, respectively. The final result is a PDF which looks the same as equation (78) or equation (81), but missing the factor of $1/\eta$ which transforms the Lagrangian PDF $Q(\eta)$ into the Eulerian PDF $P(\eta)$. So, for example, the final $P(\eta)$ for the Eulerian version of the "exact" approximation smoothed with a tophat window function for $n = -1$ is simply obtained by multiplying equation (82) by η:

$$P(\eta)d\eta = \frac{1}{2\sqrt{2\pi}\sigma_l}[(\frac{\eta}{N})^{-2/3} + (\frac{\eta}{N})^{-4/3}] \exp\Big(-\frac{9}{8\sigma_l^2}[(\frac{\eta}{N})^{1/3} - (\frac{\eta}{N})^{-1/3}]^2\Big)\frac{d\eta}{N} \tag{84}$$

where the normalization factor is now given by:

$$N = \int_{-\infty}^{\infty} \frac{1}{\sqrt{2\pi}\sigma_l} e^{-\delta_l^2/2\sigma_l^2} \left[\frac{1}{3}\delta_l + \sqrt{1+\frac{\delta_l^2}{9}}\right]^{3} d\delta_l \tag{85}$$

rather than the expression in equation (83). This Eulerian approximation is compared with the numerical results for $\sigma_l = 0.5$ in Figure 4. The agreement between this approximation and the numerical simulations is excellent. It may seem implausible that both the Eulerian and Lagrangian local mappings could produce nearly the same final $P(\eta)$, since the distributions given by equations (82) and (84) differ by a factor of η. However, this difference is compensated by the different values for N used in the two equations. In fact, our argument in the appendix indicates that these two approximations should give equally good agreement with the evolved PDF in the limit where $\sigma_l \ll 1$.

Now consider the evolution of non-Gaussian initial conditions. Our approximation can be applied in an elementary way to any initial density distribution, but there are an infinite set of distributions to choose from. To explore the differences which the initial skewness and kurtosis make in the evolution, we have chosen four representative distributions; one each with positive and negative skewness, and two symmetric (zero skewness) distributions with positive and negative kurtosis. The distributions we examine below represent some extreme cases and are not physically motivated. However, they give a general idea of the effects of positive and negative skewness or kurtosis on the evolution of the PDF.

We will consider only the smoothed exact approximation with $\sigma_l \leq 0.75$, which we know produces results in good agreement with the true PDF for the Gaussian case, and for definiteness we will take $n = -1$. For this case, the mapping in equation (80) becomes

$$\delta_l = \frac{3}{2}\Big[(\frac{\eta}{N})^{1/3} - (\frac{\eta}{N})^{-1/3}\Big], \tag{86}$$

with N given by:

$$N = \int_{-\infty}^{\infty} P(\delta_l)\left[\frac{1}{3}\delta_l + \sqrt{1 + \frac{\delta_l^2}{9}}\right]^{-3} d\delta_l, \tag{87}$$

where $P(\delta_l)$ is the initial (non-Gaussian) distribution which we are evolving.

For the case of positive skewness, a simple choice is the gamma distribution with zero mean and variance σ_l^2:

$$P(\delta_l)d\delta_l = \frac{\nu^{\nu/2}}{\Gamma(\nu)\sigma_l}(\frac{\delta_l}{\sigma_l} + \sqrt{\nu})^{\nu-1} e^{-\nu-\sqrt{\nu}\delta_l/\sigma_l} d\delta_l, \tag{88}$$

where each value of ν defines a different gamma distribution. A mirror image negative skewness distribution with zero mean can be obtained by simply changing δ_l to $-\delta_l$ in equation (88). For definiteness, we take $\nu = 3$, and our results for positive and negative initial skewness are shown in figures 5 and 6, at $\sigma_l = 0.2$, 0.5, and 0.75. Both density distributions show qualitatively the expected evolution, i.e., the development of increasing skewness and a large positive tail. For the positive skewness case (figure 5) this does not represent a major change in the shape of the distribution function. The effect is more dramatic in figure 6, where the distribution function with negative initial skewness flips into a PDF with positive skewness, as expected. Oddly, the function with negative initial skewness develops a larger tail at large η than does the function with positive initial skewness.

For symmetric distribution functions we have chosen two "extreme" representative models, the bilateral exponential:

$$P(\delta_l)d\delta_l = \frac{1}{\sqrt{2}\sigma_l} e^{-\sqrt{2}|\delta_l|/\sigma_l} d\delta_l, \tag{89}$$

which has large positive kurtosis, and the uniform distribution

$$P(\delta_l)d\delta_l = \frac{1}{2\sqrt{3}\sigma_l}d\delta_l, \quad |\delta_l| < \sqrt{3}\sigma_l, \tag{90}$$

$$= 0 \qquad \text{(otherwise)}, \tag{91}$$

with large negative kurtosis. Neither of these can be considered a realistic initial distribution, but they illustrate the effect of large kurtosis for symmetric initial conditions. The evolved PDF's for these two models are given in figure 7 (bilateral distribution) and figure 8 (uniform distribution). In both cases, the singularities in the initial density distribution remain in the evolved PDF. However, despite the extreme nature of the initial distribution functions, in both cases the evolved PDF shows the expected qualititative behavior, with increasing skewness and the development of a tail at large η.

5 CONCLUSIONS

Despite the simple-mindedness of local Lagrangian approximations, our "exact" approximation provides remarkable agreement with numerical simulations of the evolution of the density distribution function with Gaussian initial conditions. This agreement can be understood in terms of the fact that this approximation reproduces nearly exactly the hierarchical amplitudes at tree level. The planar and spherical approximations appear to bound the evolution of the PDF but are much less useful (unless, of course, one is interested in the evolution of one-dimensional density fields, in which case the planar approximation is exact for any initial conditions).

For the case of non-Gaussian initial conditions, we cannot be as confident. Unlike the case of Gaussian initial conditions, the evolution of the hierarchical amplitudes is non-local, as has been shown by Fry & Scherrer (1994) and Chodorowski & Bouchet (1996). Thus, no local approximation can exactly reproduce the hierarchial amplitudes for non-Gaussian initial conditions. However, the exact approximation does a reasonable job of reproducing the hierarchical amplitudes for limiting cases where a local approximation is valid. Furthermore, the application of this approximation to various non-Gaussian initial conditions does show reasonable agreement with the expected qualitative behavior.

The mapping which gives us the exact approximation can also be applied backwards, to map the evolved distribution function back onto the initial distribution function. This procedure is guaranteed to produce the correct initial distribution function only for the case of Gaussian initial conditions, and only for reasonably small σ_l, but it is obvious from Fig. 1a that it would be highly accurate in this case. This method should, in principle, be capable of distinguishing Gaussian from non-Gaussian initial conditions, even if it could not accurately give the exact form of the latter.

We thank Josh Frieman for helpful discussions. We are grateful to David Weinberg for providing us with results of his gravitational clustering simulations. R.J.S. was supported in part by the Department of Energy (DE-AC02-76ER01545). Z.A.M.P. and R.J.S were supported in part by NASA (NAG 5-2864).

APPENDIX: The Vertex Generating Function for Local Approximations

Here we demonstrate the simple form of the vertex generating function for local Lagrangian approximations applied to Gaussian initial conditions; namely, for a local Lagrangian mapping $\eta = N(t)f(\delta_l)$, where $N(t)$ is a function only of σ_l, the vertex generating function is given by

$$G_\delta(\tau) = f(\delta_l) - 1 \tag{92}$$

Our argument proceeds in two stages. First we show that this relation holds for the simpler case of local Eulerian mappings. Then we show that the vertex generating function is the same for local Eulerian and local Lagrangian mappings.

Consider first the local Eulerian approximation

$$\eta(\mathbf{x}) = N_E(t)f(\delta_l(\mathbf{x})). \tag{93}$$

The mapping f can be expanded in a power series

$$f(\delta_l) = \sum_{j=0}^{\infty} b_j \delta_l^j \tag{94}$$

where $b_0 = 1$, and $N(t)$, for Gaussian initial conditions, can be a function only of σ_l:

$$N_E(t) = \sum_{k=0}^{\infty} c_k \sigma_l^k. \tag{95}$$

where $c_0 = 1$. These three equations give us the expression for the n^{th} order expansion of δ:

$$\delta^{(n)} = \sum_{j+k=n} b_j c_k \delta_l^j \sigma^k. \tag{96}$$

We can substitute this expression into equation (43) to obtain ν_n. When we do this and take the connected average, all of the terms vanish except for the term $j = n$, $k = 0$; the other terms are not connected. The final result is

$$\begin{aligned} \nu_n &= \frac{\int \langle b_n \delta^{(1)^n}(\mathbf{x})\delta^{(1)}(\mathbf{x}_1)...\delta^{(1)}(\mathbf{x}_n)\rangle_c d^3\mathbf{x}\ d^3\mathbf{x}_1...d^3\mathbf{x}_n}{(\int \langle \delta^{(1)}(\mathbf{x})\delta^{(1)}(\mathbf{x}')\rangle d^3\mathbf{x}\ d^3\mathbf{x}')^n} \\ &= b_n n! \end{aligned} \tag{97}$$

since there are $n!$ different connected graphs. Then from equation (42) we obtain

$$\begin{aligned} G_\delta(\tau) &= \sum_{n=1}^{\infty} b_n \tau^n \\ &= f(\tau) - 1 \end{aligned} \tag{98}$$

Thus, equation (45) holds for local Eulerian mappings; we now show that $G_\delta(\tau)$ is the same if we take $f(\delta_l)$ to be a local Lagrangian mapping instead of a local Eulerian mapping. To do this, we first note that G_δ is completely determined by the values of ν_n (equation 42), which are, in turn, completely determined by the $S_p(0)$'s (equation 44). Thus, it suffices to show that the local Eulerian mapping given by equation (93) and the local Lagrangian mapping

$$\eta(\mathbf{q}) = N_L(t)f(\delta_l(\mathbf{q})) \tag{99}$$

have the same values for $S_p(0)$, which is equivalent to the statement that they have identical cumulants κ_p in the limit $\sigma \to 0$.

To demonstrate this, we introduce the characteristic function $\phi_E(t)$ for the Eulerian mapping, which is the Fourier transform of the PDF:

$$\phi_E(t) = \int P_E(\eta) e^{i\eta t} d\eta \tag{100}$$

where we assume that $P_E(\eta)$ is the PDF for the Eulerian mapping given by equation (93). If instead we use the same function to produce the local Lagrangian mapping given by equation (99), we obtain the PDF $P_L(\eta)$, with corresponding characteristic function $\phi_L(t)$. Using equation (18) for the Lagrangian mapping, and its equivalent (without the $1/\eta$ factor) for the Eulerian mapping, we find that ϕ_L and ϕ_E are related by:

$$\phi_E(\frac{N_L}{N_E}t) = \frac{1}{i}\phi_L'(t), \tag{101}$$

where N_L and N_E are the normalizing factors for the Lagrangian and Eulerian mappings, given respectively by

$$N_L = \langle \frac{1}{f(\delta_l)} \rangle \tag{102}$$

and

$$N_E = \frac{1}{\langle f(\delta_l) \rangle}. \tag{103}$$

The cumulants we wish to calculate are related to the characteristic function by

$$\phi(t) = \exp(\sum_{p=1}^{\infty} \frac{(it)^p}{p!}\kappa_p) \tag{104}$$

If we let $\kappa_p^{(E)}$ represent the cumulants for the Eulerian mapping, and $\kappa_p^{(L)}$ represent the cumulants for the Lagrangian mapping, then we can substitute equation (104) into equation (101) to obtain:

$$\sum_{p=1}^{\infty} [\kappa_p^{(E)} (\langle f \rangle \langle 1/f \rangle)^p - \kappa_p^{(L)}] \frac{(it)^p}{p!} = \ln[1 + \sum_{p=1}^{\infty} \kappa_{p+1}^{(L)} \frac{(it)^p}{p!}], \tag{105}$$

where we have used the fact that $\kappa_1^{(L)} = 1$. Now we note that for both the Eulerian and Lagrangian mappings considered here, the "evolved" distribution is hierarchical, so that $\kappa_p^{(L)} \sim O(\sigma^{2(p-1)})$, and $\kappa_p^{(E)} \sim O(\sigma^{2(p-1)})$. Furthermore, $(\langle f \rangle \langle 1/f \rangle)^p = 1 + O(\sigma^2)$. Expanding out the right-hand side of equation (105) and equating terms with equal powers of t^p, we find that

$$\kappa_p^{(E)} - \kappa_p^{(L)} \sim O(\sigma^{2p}). \tag{106}$$

Furthermore, κ_p for $P(\eta)$ and κ_p for $P(\delta)$ are identical for $p > 1$, since η and δ differ by a constant. Thus, the difference between $S_p(\sigma)$ for the Lagrangian local mapping and $S_p(\sigma)$ for the local Eulerian mapping vanishes in the limit where $\sigma \to 0$, so that the two mappings have the same $G_\delta(\tau)$.

These results allow us to generate, in a simple way, two different mappings which, when applied to Gaussian initial conditions, yield a density field with any desired vertex generating function $G_\delta(\tau)$ or hierarchical amplitudes $S_p(0)$.

REFERENCES

Bernardeau, F., 1992, ApJ, 392, 1
Bernardeau, F., 1994, A & A, 291, 697
Bernardeau, F., & Kofman, L., 1995, ApJ, 443, 479
Betancort-Rijo, J., 1991, MNRAS, 251, 399
Chodorowski, M.J., & Bouchet, F.R., 1996, MNRAS, in press
Coles, P., Moscardini, L., Lucchin, F., Matarrese, S., & Messina, A. 1993, MNRAS, 264, 749
Fry, J.N., 1984, ApJ, 279, 499
Fry, J.N., & Scherrer, R.J., 1994, ApJ, 429, 36
Juszkiewicz, R., Weinberg, D.H., Amsterdamski, P., Chodorowski, M., & Bouchet, F., 1995, ApJ, 442, 39
Kofman, L., 1991, in Primordial Nucleosynthesis and Evolution of Early Universe, Ed. K. Sato & J. Audouze (Dordrecht: Kluwer), 495
Kofman, L., Bertschinger, E., Gelb, J.M., Nusser, A., & Dekel, A., 1994, ApJ, 420, 44
Lokas, E.L., Juszkiewicz, R., Bouchet, F.R., & Hivon, E. 1996, ApJ, in press
Lokas, E.L., Juszkiewicz, R., Weinberg, D.H., & Bouchet, F.R. 1995, MNRAS, 274, 730
Matarrese, S., Lucchin, F., Messina, A., & Moscardini L. 1991, MNRAS, 253, 35
Matarrese, S., Lucchin, F., Moscardini, L., & Saez, D. 1992, MNRAS, 259, 437
Messina, A., Moscardini, L., Lucchin, F., & Matarrese, S. 1990, MNRAS, 245, 244
Moscardini, L., Matarrese, S., Lucchin, F., & Messina A. 1991, MNRAS, 248, 424
Munshi, D., Sahni, V., & Starobinsky, A.A. 1994, ApJ, 436, 517
Nusser, A., Dekel, A., Bertschinger, E., & Blumenthal, G.R. 1991, ApJ, 379, 6
Padmanabhan, T., & Subramanian, K. 1993, ApJ, 410, 482
Peebles, P.J.E. 1980, The Large-Scale Structure of the Universe (Princeton University Press)
Sahni, V., & Coles, P. 1995, Phys. Rep., 262, 1
Scoccimarro, R. & Frieman, J. 1996, ApJ, submitted
Shandarin, S.F., & Zel'dovich, Ya. B. 1989, Rev Mod Phys, 61, 185
Stuart, A., & Ord, J.K. 1987, Kendall's Advanced Theory of Statistics, Vol. 1 (London: Charles Griffin)
Weinberg, D.H., & Cole, S. 1992, MNRAS, 259, 652
Zel'dovich, Ya.B. 1970, A & A, 5, 84

FIGURE CAPTIONS

Figure 1: Comparison of our exact approximation for the evolution of the smoothed density distribution function (solid curve) with the results of a numerical simulation of gravitational clustering (points with error bars), for Gaussian initial conditions with power spectrum $P(k) \propto k^{-1}$ and spherical top-hat smoothing. The distribution functions are calculated for a linearly evolved rms fluctuation of (a) $\sigma_l = 0.5$, (b) $\sigma_l = 0.75$, (c) $\sigma_l = 1.0$.

Figure 2: As Figure 1, but here the results of the numerical simulation of gravitational clustering (points with error bars) are compared with the smoothed density distributions given by the planar approximation (dotted curve) and the spherical approximation (dashed curve) for (a) $\sigma_l = 0.5$, (b) $\sigma_l = 0.75$.

Figure 3: As Figure 1, but here the results of the numerical simulation of gravitational clustering (points with error bars) are compared with the unsmoothed density distributions given by the exact approximation (solid curve), the planar approximation (dotted curve), and the spherical approximation (dashed curve), for $\sigma_l = 0.5$.

Figure 4: As Figure 1a, using an Eulerian version of the exact approximation (solid curve).

Figure 5: Evolved smoothed density distribution functions given by the exact approximation with $P(k) \propto k^{-1}$, for an initial gamma function density distribution with positive skewness. The distribution functions are calculated for a linearly evolved rms fluctuation of $\sigma_l = 0.2$ (solid curve), $\sigma_l = 0.5$ (dashed curve), and $\sigma_l = 0.75$ (dotted curve).

Figure 6: As Figure 5, for an initial gamma function with negative skewness.

Figure 7: As Figure 5, for an initial bilateral exponential function.

Figure 8: As Figure 5, for an initial uniform distribution.

Fig. 1a

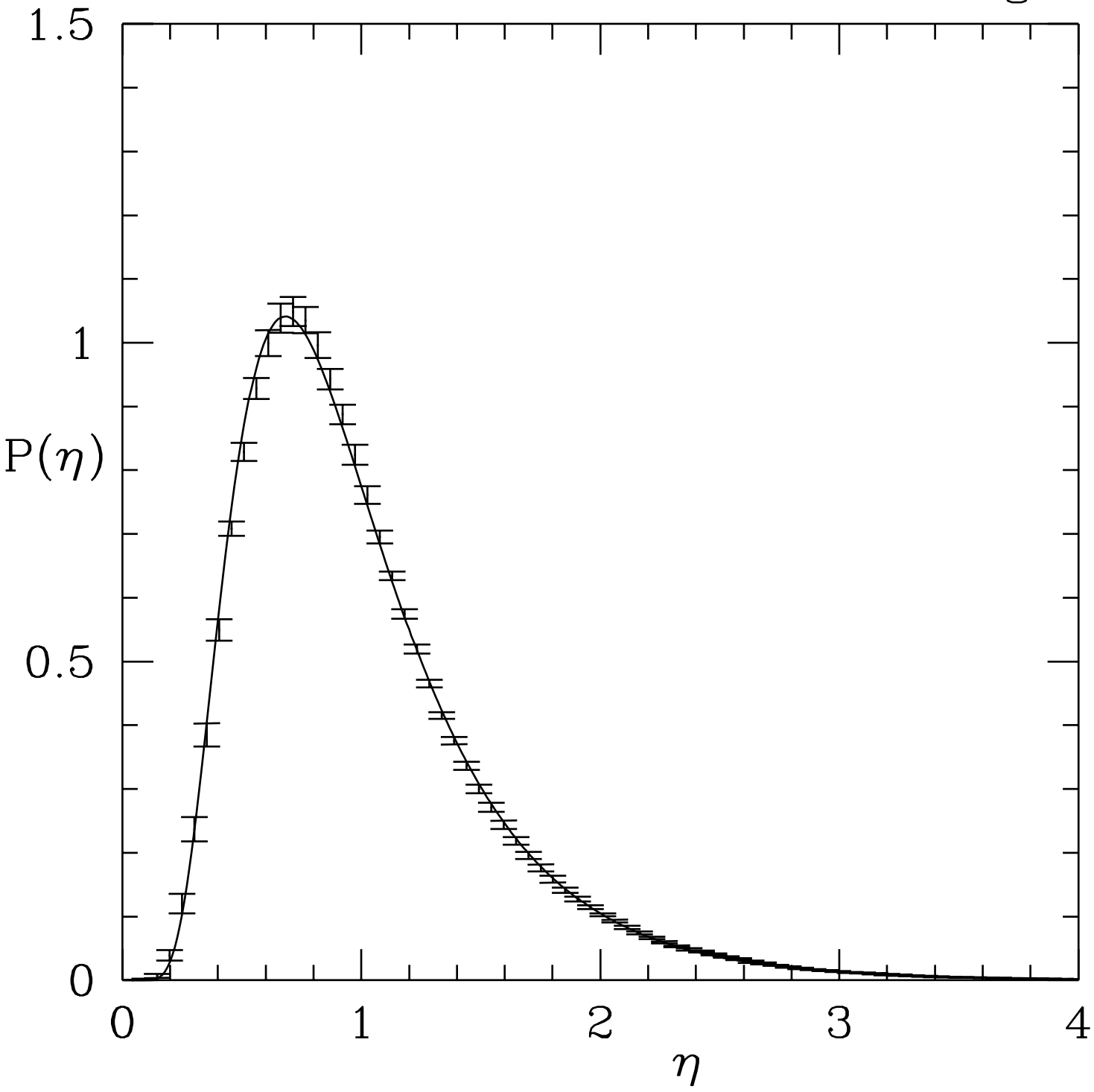

Fig. 1b

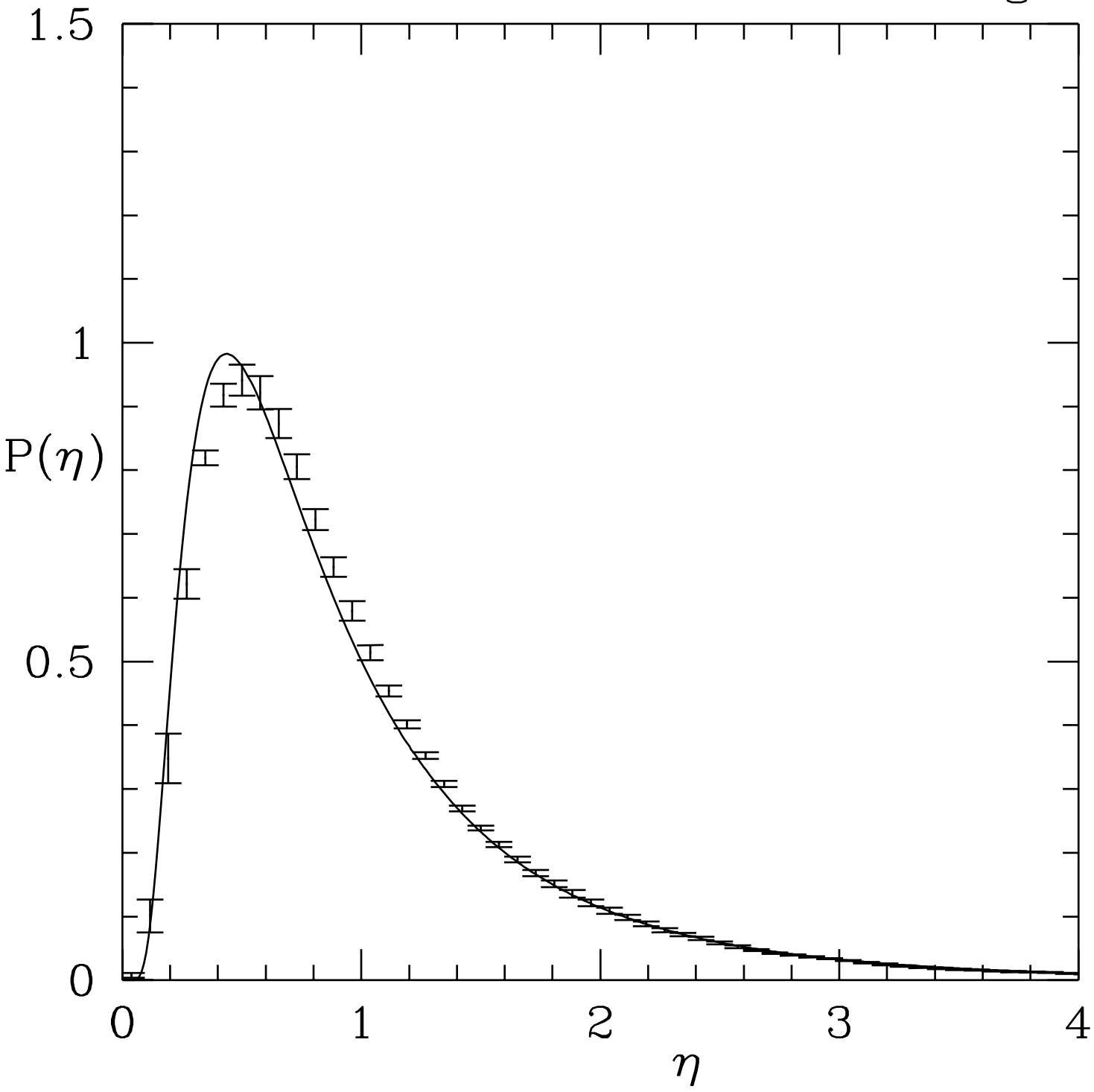

Fig. 1c

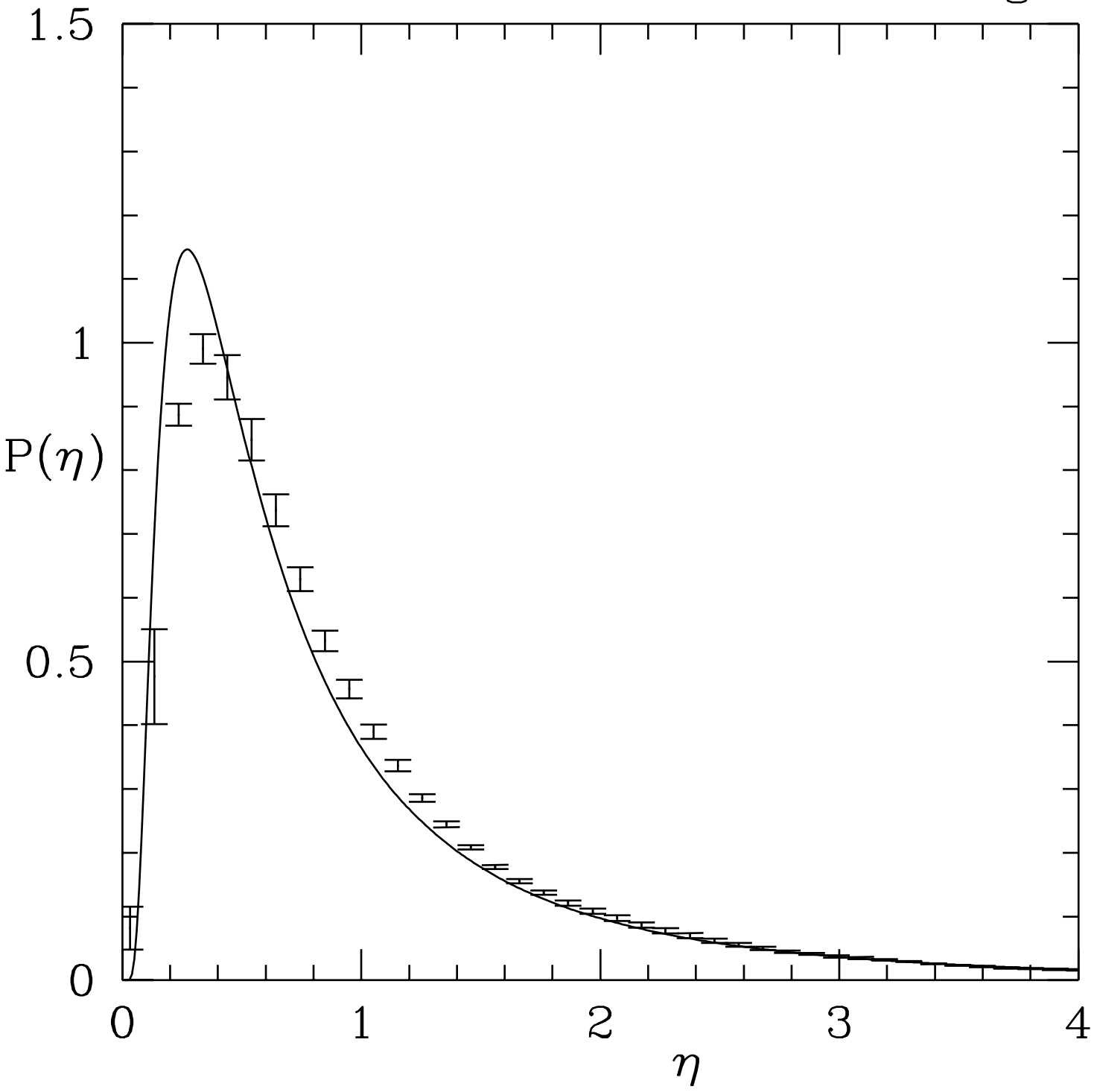

Fig. 2a

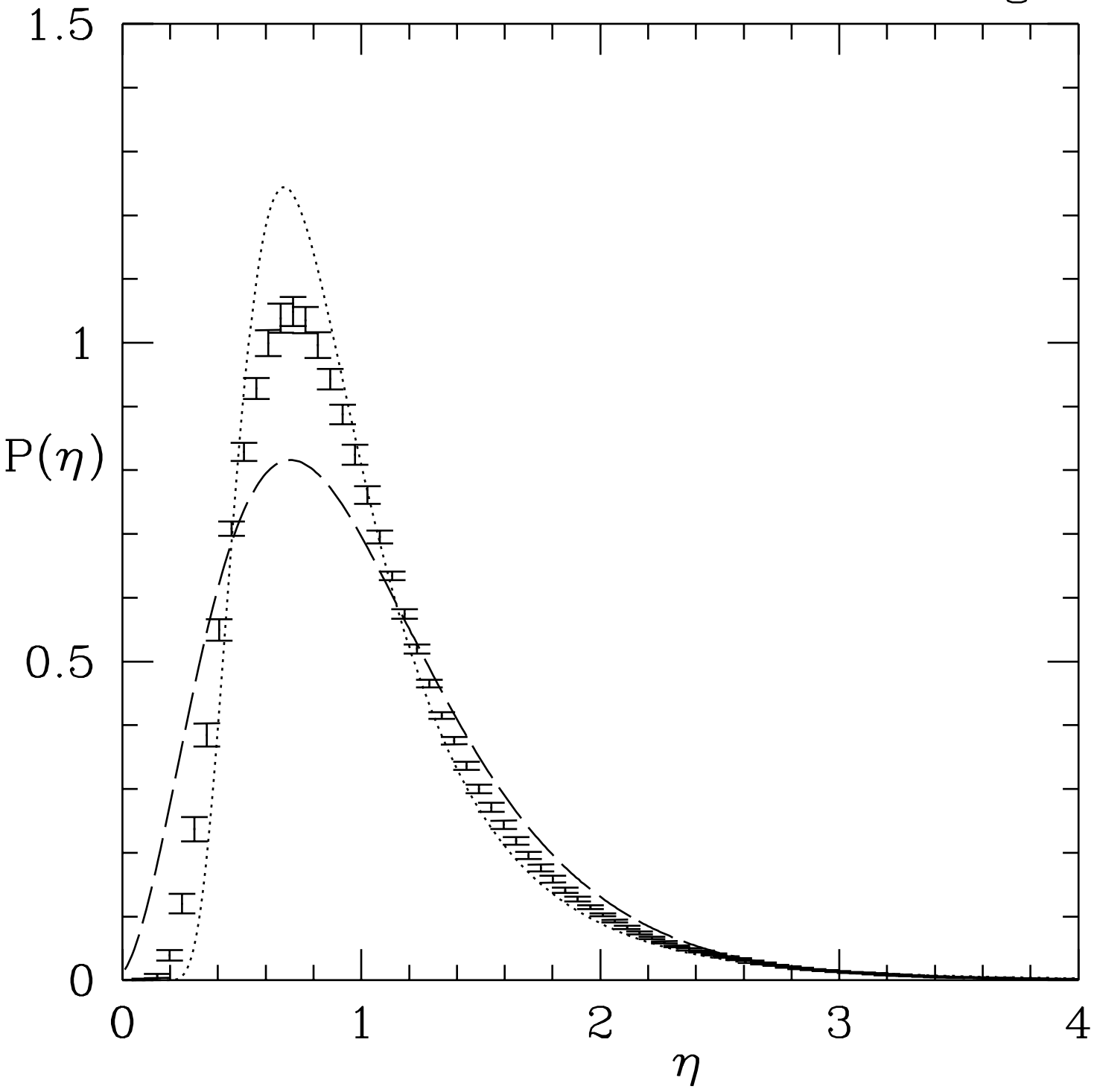

Fig. 2b

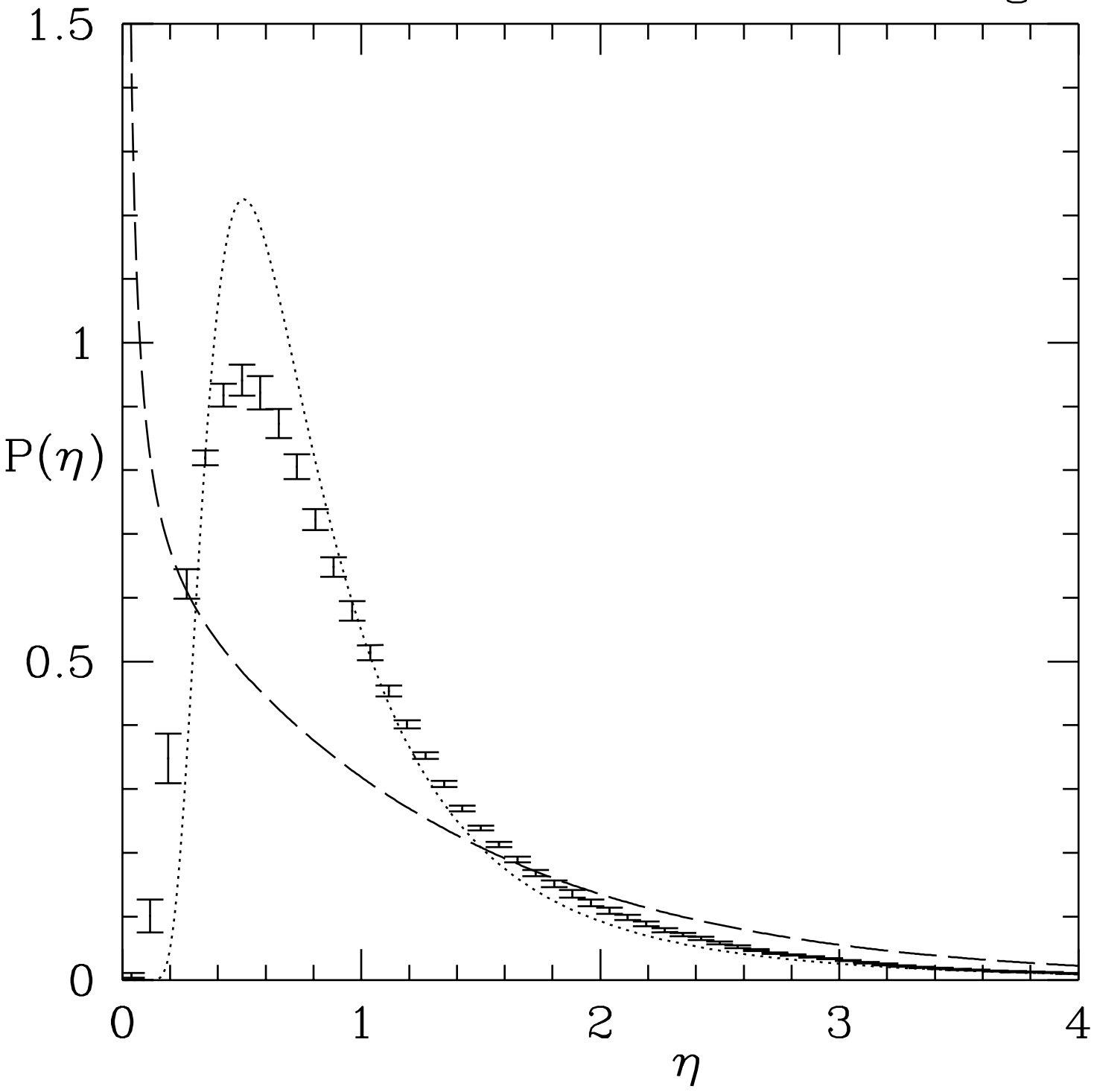

Fig. 3

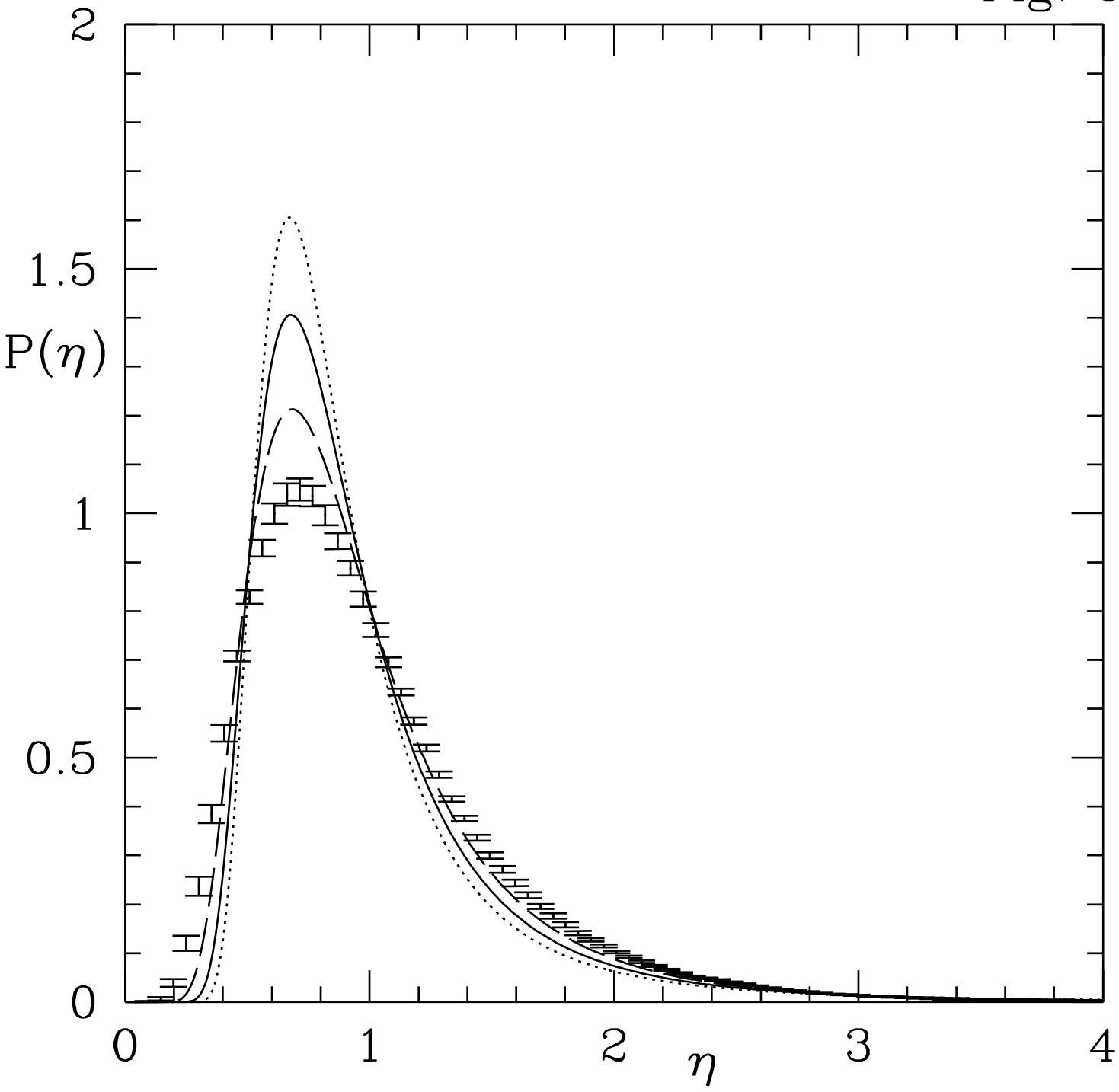

Fig. 4

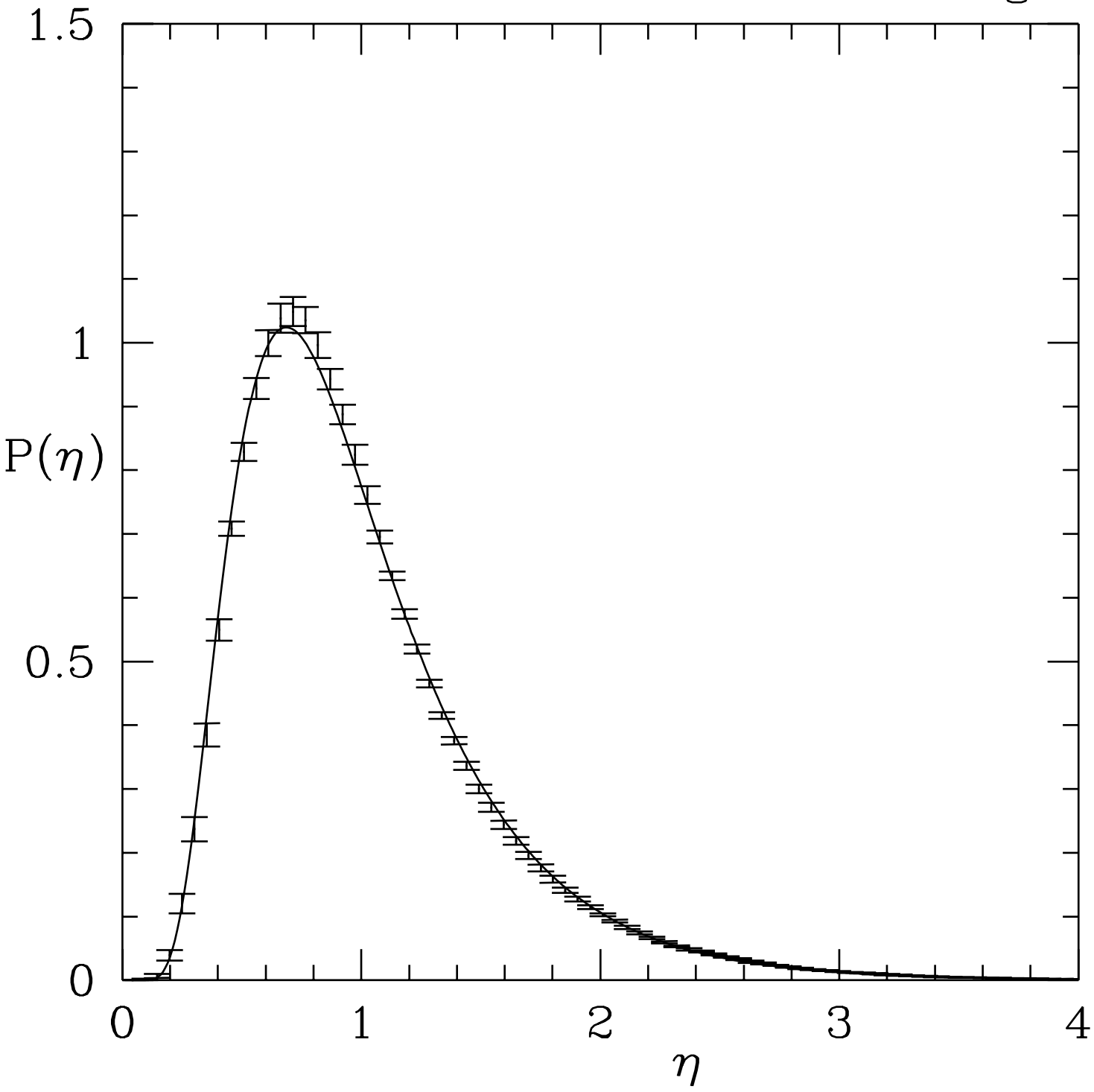

Fig. 5

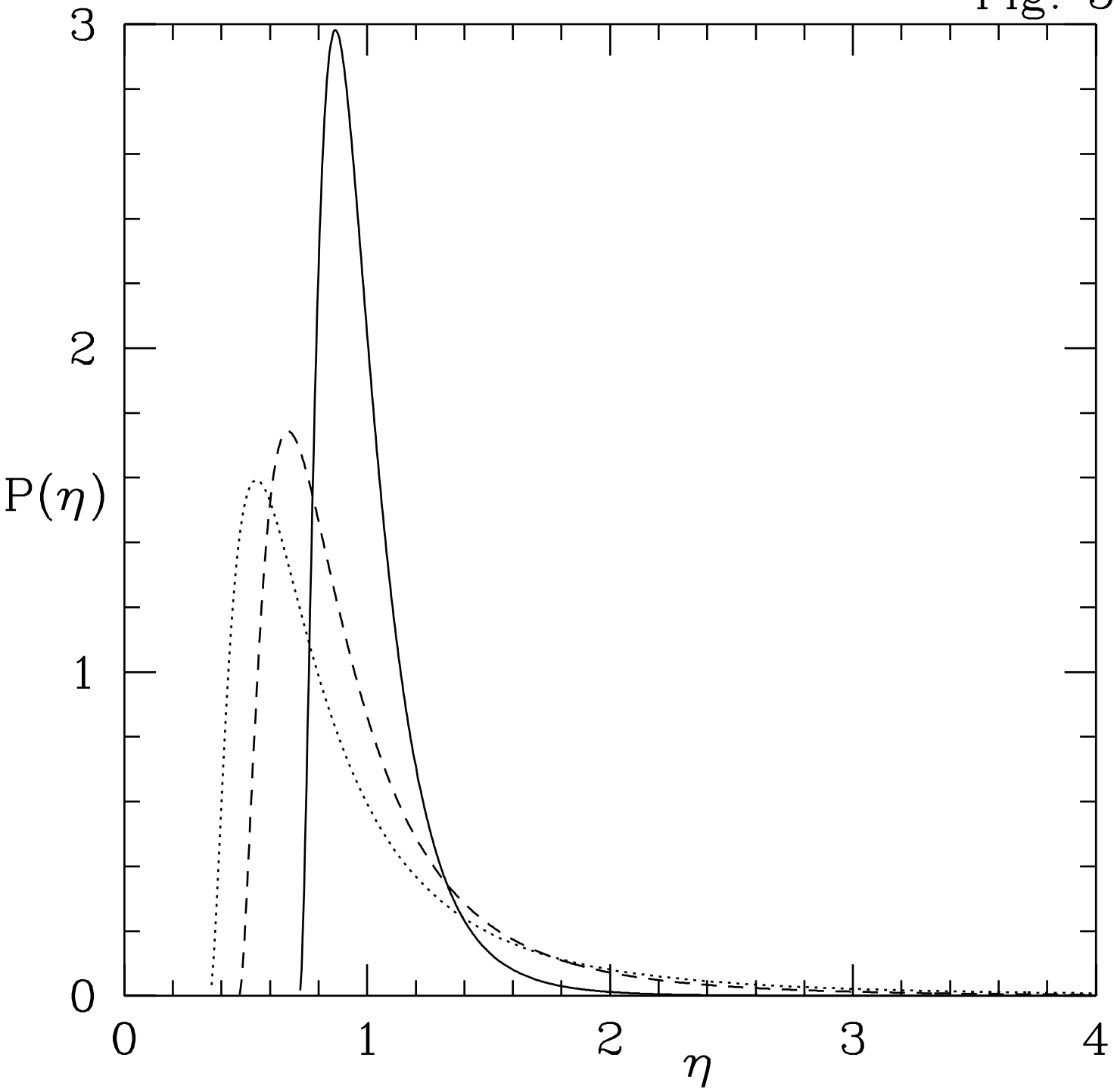

Fig. 6

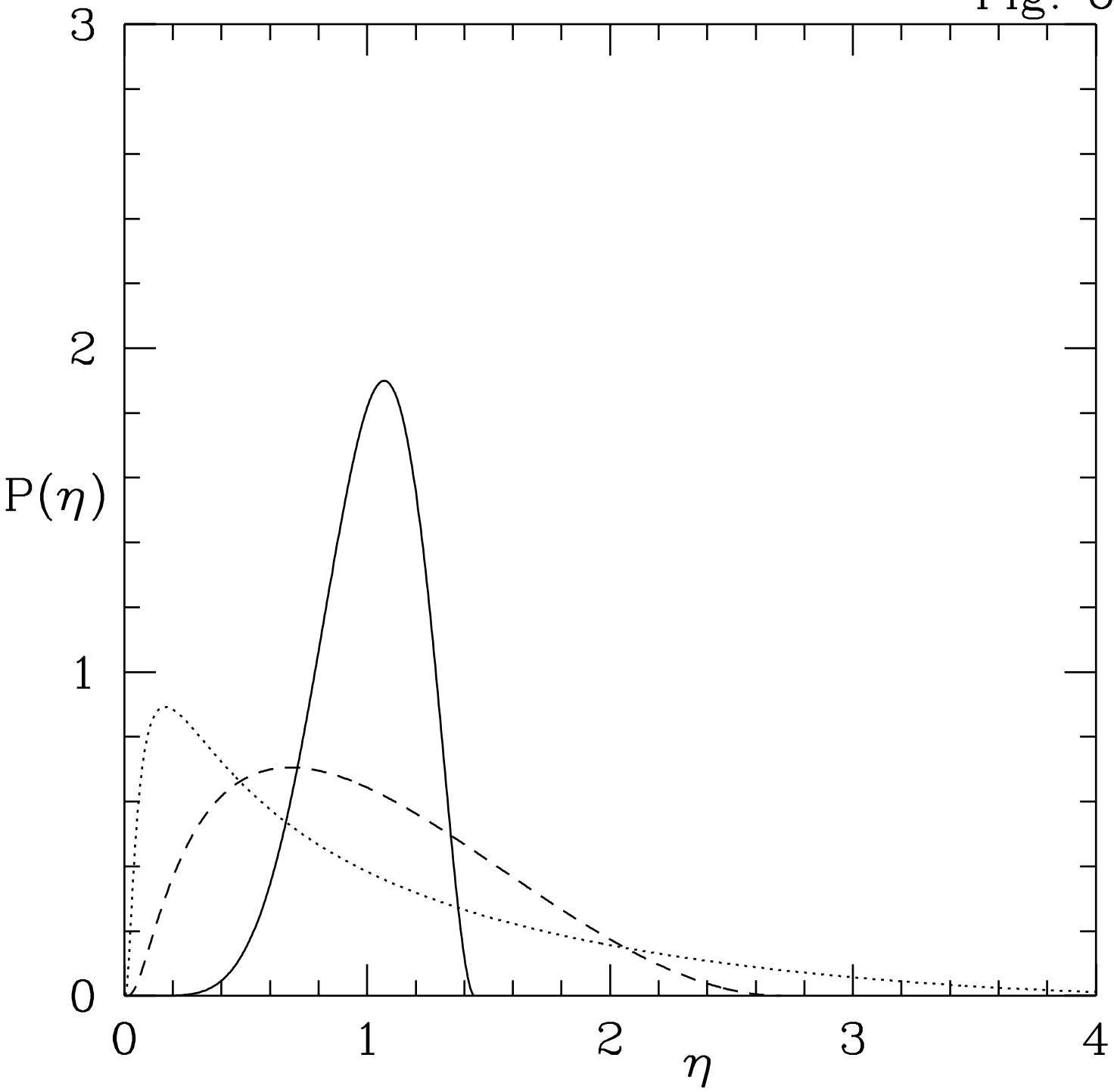

Fig. 7

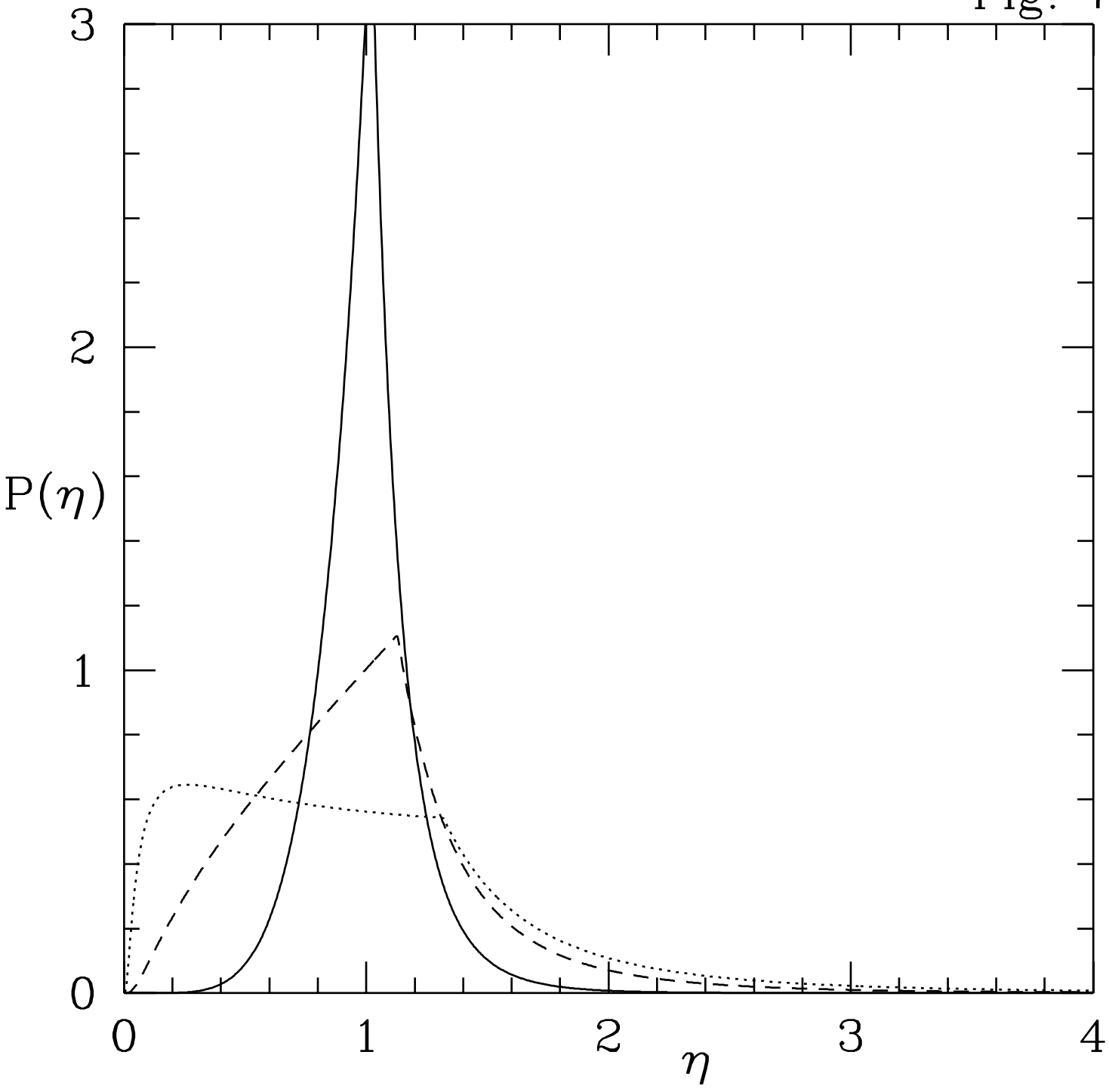

Fig. 8